

Spatial partitioning: spatial clusters and boundary detection

Introduction

In order to understand ecological processes at multiple scales, ecological studies are often carried out over large regions (see Chapter 8). By doing so, most study areas include ecological processes that can act at different spatial and temporal scales (Dungan *et al.* 2002). In such cases, it is unlikely that the standard assumption of stationarity (i.e. the same mean, variance and isotropy; see Chapters 1 and 2) is valid. To analyse ecological data from large regions in a meaningful way, the region should therefore be partitioned into smaller, more homogeneous areas (i.e. patches) that are more likely to be governed by the same ecological process and hence stationary. Stratifying a region can also be useful for monitoring and managing resources by informing locally appropriate adjustments. There are two main approaches to spatially partition a region:

- (1) grouping adjacent locations that have similar values of the indicator variable(s) by generating spatial clusters (Figure 9.1), or
- (2) dividing the whole region into subareas, based on their degree of dissimilarity, by delineating boundaries between different areas (Figure 9.2).

In theory, the outcomes of these two approaches should give the same partitioning between sampling locations. In practice, however, there may be more or less pronounced mismatches between the two methods. This is mostly because the majority of the partitioning methods are descriptive and somewhat subjective in their application and interpretation.

In this chapter, we present the spatial partitioning methods, ranging from spatial clustering to boundary detection, which are most relevant to ecologists (Figure 9.3). Edge or boundary detection is an important area of research in computer vision and image analysis, with applications in remote sensing and medicine. Here we will concentrate on the analytic tools that are most appropriate for ecological data and questions.

9.1 Patch identification

9.1.1 Patch properties

A patch can be defined as a spatially homogeneous area throughout which at least one variable has similar attributes either of a category (e.g. 'forested' rather than 'crop') or of a quantitative value (e.g. average tree age). Consequently, adjacent patches are different from one another for at least one variable. The juxtaposition of patches creates a mosaic in which each patch can be characterized by its structural properties such as area (e.g. small, large), shape (e.g. elliptic, square, sinuous, etc.), boundary properties (e.g. sharp, gradual; see Section 9.2.1), and the contrast between adjacent patches (e.g. low between deciduous forest and mixed forest; high between forest and agriculture crop). Many patch properties can be computed using landscape metrics (Li & Reynolds 1995; Gustafson 1998; Tischendorf 2001; Fortin *et al.* 2003; Turner *et al.* 2003; Remmel & Fortin 2013). The above definition of patches is data-driven and implies that

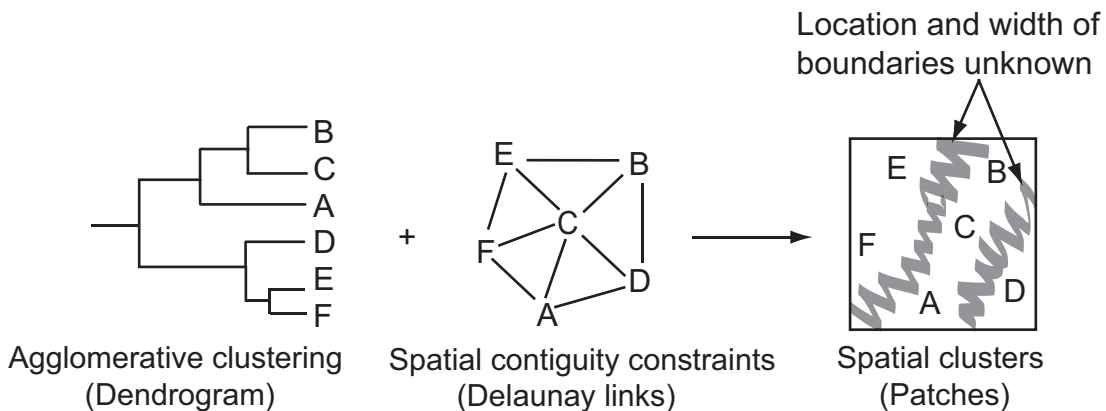


Figure 9.1 Spatial clustering where clusters are formed only when the degree of similarity between sampling locations (A, B, C, D, and E), as determined by the algorithm (here an agglomerative one), is high, and where the sampling locations are adjacent to one another (e.g. A is adjacent to F, C, and D) in a chosen spatial connectivity structure (here Delaunay links). The exact location and width of the boundaries between the spatial clusters are not determined by this method, as illustrated by the grey zigzags. In fact, the spatial clustering algorithm only identifies the membership of each sampling location to a spatial cluster.

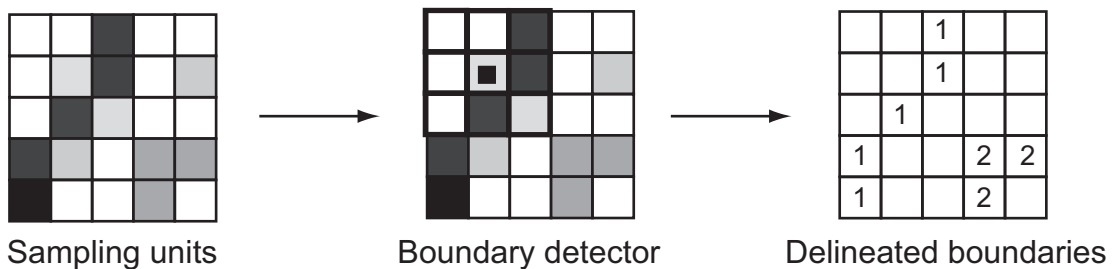


Figure 9.2 Boundary detection using a kernel (see Section 9.2), where the 1s indicate the locations where boundaries are the most pronounced (sharp) and the 2s the second most pronounced boundaries. The grey shades correspond to quantitative values of a variable (low, black; high, white).

the spatial distribution of the values of targeted variable(s) is more-or-less uniform. This does not imply that all the variables measured in a given patch have a spatially uniform distribution. Similarly, when patches are arbitrarily delineated, as political or administrative units often are, the within-patch spatial structure of the data can range from a weak monotonic trend to strong spatial autocorrelation. The presence of within-patch spatial structure can reduce our ability to delineate boundaries accurately (Burrough & Frank 1996; Csillag *et al.* 2001; Edwards & Fortin 2001; Jacquez *et al.* 2008; Philibert *et al.* 2008).

9.1.2 Spatial clustering

Patches are in essence spatial clusters of sampling locations based on both their spatial adjacency and similarity in term of the values of the measured variable(s). Clusters are usually based on the degree of similarity between data at different locations and there are many clustering algorithms that generate clusters (see Legendre & Legendre (2012) for a complete review and mathematical details). The clustering algorithms most commonly used are hierarchical agglomerative methods (e.g. single, intermediate, and

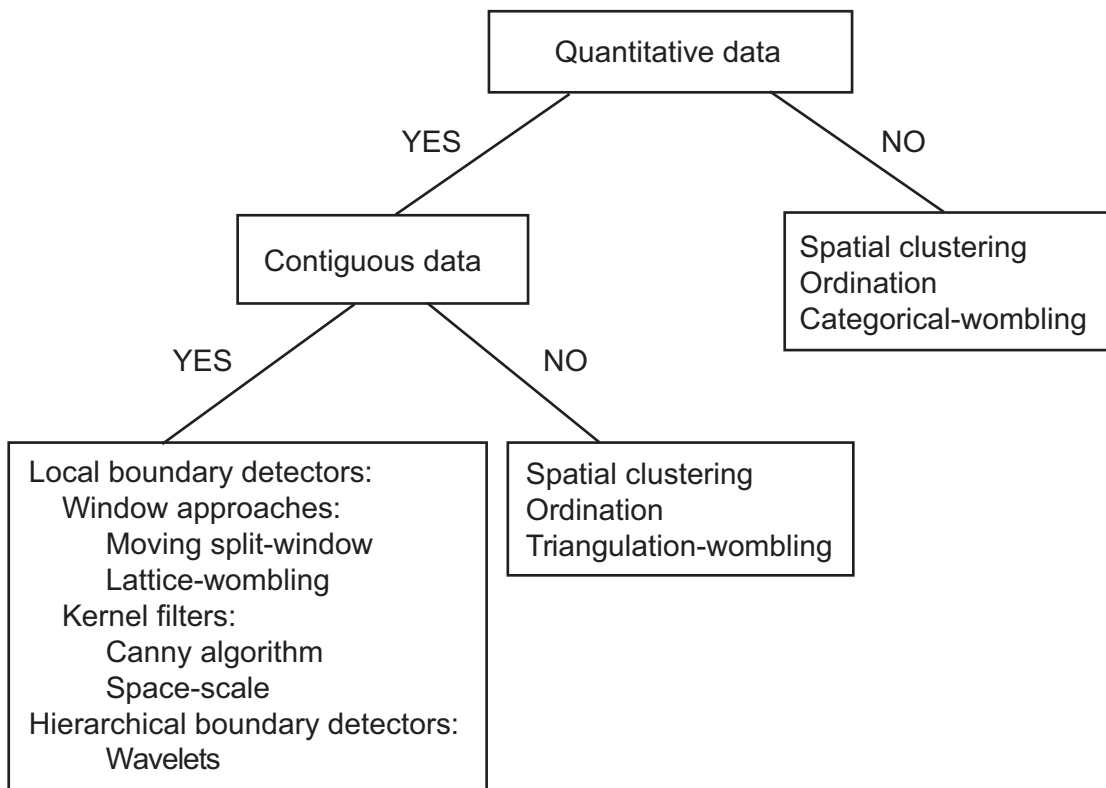


Figure 9.3 Decision tree to guide the selection of boundary detection methods for ecological data.

complete linkage, as well as centroid). Hierarchical agglomerative methods start with all sampling locations separated and then merge them into larger groups based on the degree of similarity among the locations forming clusters. To address the particular nature of ecological data (e.g. presence : absence data, rare species, the double-zeros of dual absences), many similarity and dissimilarity metrics have been developed (Legendre & Legendre 2012). The researcher can define a priori the degree of similarity at which samples are merged into an existing cluster. The linkage family of methods can be described as a gradient of criteria that need to be met before a sampling location can merge into a group, for example, in single linkage two sampling locations or clusters merge based on the minimum distance (or maximum similarity) between them;

in intermediate linkage, the similarity of a sampling location or cluster is compared to all possible pairs in the existing cluster before merging; and in complete linkage, the merging of clusters occurs when the maximum distance (or minimum similarity) between clusters is reached. The centroid algorithm is comparable to the intermediate-linkage example where a sampling location merges with a cluster when its similarity value is comparable to the centroid value of the cluster. The advantage of agglomerative clustering procedures is that they create non-overlapping clusters. Several papers and books report the subtleties of clustering methods (e.g. Legendre & Legendre 2012). The most important drawback is the subjectivity involved in the selection of the degree of similarity for the creation of clusters.

Clustering can also be achieved using another type of algorithm known as the *k*-means partitioning algorithm. The *k*-means algorithm requires that the user decides a priori the number of clusters to be formed. Then the *k*-means algorithm optimizes using an iterative process in which sampling locations cluster, minimizing the within-cluster sum of squares error and maximizing the similarity of each sample to the centroid of the cluster to which it belongs. In this method, some subjectivity arises in the choice of the number of clusters.

To create spatial clusters, spatial constraints among the sampling locations need to be added in the clustering algorithm (Legendre & Fortin 1989). Spatial adjacency among sampling locations can be determined from any of the connectivity structures or neighbour networks presented in Chapter 3. Then spatial clusters are formed by merging spatially adjacent sampling locations that have comparable values (Figure 9.1). A by-product of forming spatial clusters is that there are 'boundaries' between them (Figure 9.1), but their exact location and width are unknown. This is the weakness of these spatial clustering methods: the sampling locations have a known cluster membership but the location of the boundaries between the spatial clusters is unknown.

Spatial clustering methods are yet very valuable approaches as spatial clusters can be obtained for any data type (qualitative or quantitative, univariate or multivariate) sampled with any design (contiguous sampling units or not; Figure 9.3). There are still two major problems with spatial clustering methods.

- (1) In the absence of a priori knowledge, or independent information about the ecological data, the researcher needs to select either the level of similarity for the agglomerative algorithms or the number of spatial clusters for *k*-means partitioning at which the spatial clusters will be obtained and subsequently interpreted ecologically. To achieve this, Gordon (1999) developed a goodness-of-fit index, *G*, that indicates how the number of clusters selected contributes to minimizing the sum of squares error of the between-clusters variability, *B*, when compared to the within-clusters variability, *W*:

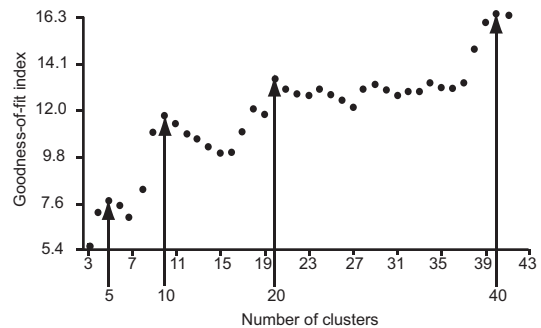


Figure 9.4 Goodness-of-fit index values according to the number of spatial clusters. The higher the index, the higher the contrast between the within-patch and among-patch sum of errors. Here, we are interested in the best number of spatial clusters to partition a study area having 84 sampling locations (a 6×14 grid) based on tree abundance data (Fortin 1992). For comparison purposes, we selected four numbers of clusters: 5, 10, 20 and 40 (see Figure 9.5).

$$G = [B/(k-1)] \div [W/(n-k)], \quad (9.1)$$

where *k* is the number of clusters and *n* is the number of sampling locations. The value of this goodness-of-fit index is therefore a guide to the appropriate number of clusters. It is important to have an underlying ecological question to provide an upper limit to the number of clusters requested. The choice of the appropriate number of clusters to select should therefore be guided by the goal of the research and knowledge about the study area.

For example, the 'best partition' in terms of spatial clusters of forest canopy composition (based on the abundance of 26 tree species in 10×10 m sampling units; Fortin 1997) is obtained using 40 spatial clusters (i.e. the highest value of goodness-of-fit as illustrated in Figure 9.4). This is a large number of spatial clusters for only 84 sampling locations. Based on our knowledge of the study area (Fortin 1992), three to five spatial clusters should be able to describe the spatial arrangement of the woodlot tree canopy. For comparison, however, we selected four values where the numbers of clusters show a local maximum in the goodness-of-fit index value: 5, 10, 20 and 40. In Figure 9.5, the spatial layout of the clusters

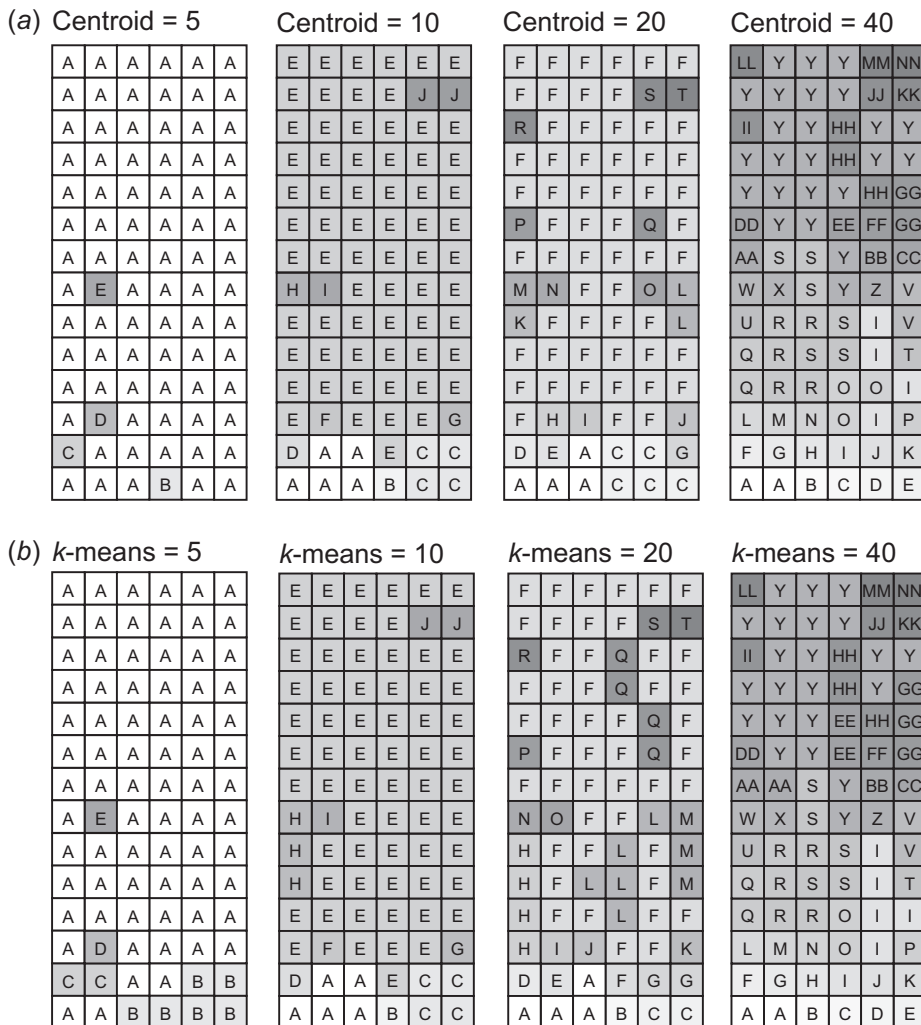


Figure 9.5 Spatial clusters on the tree abundance data of 84 sampling locations based on Delaunay connection links and (a) the centroid agglomerative algorithm and (b) the *k*-means method. Spatial partitions based on five spatial clusters identify that most of the spatial heterogeneity is concentrated in the lower left part of the study area and there is some heterogeneity in the middle of the plot. Spatial partitions based on 10 and 20 spatial clusters divide the large spatial cluster A, based on five spatial clusters, into smaller spatial clusters stressing much spatial heterogeneity over the entire plot. For spatial partitions based on 40 spatial clusters, although the number of clusters provided the highest goodness-of-fit index value, several spatial clusters were created having only one or two sampling locations. Overall, the *k*-means clustering algorithm creates larger spatial clusters than the agglomerative one.

based on different clustering algorithms (hierarchical agglomerative centroid and *k*-means and number of clusters (5, 10, 20 and 40)) can be compared visually. In doing so, we observe that

both clustering algorithms provide similar spatial clusters, but the agglomerative algorithm creates more clusters of only one sampling location (4 out of 5; 6 out of 10; 15 out of 20; 30 out of 40) than

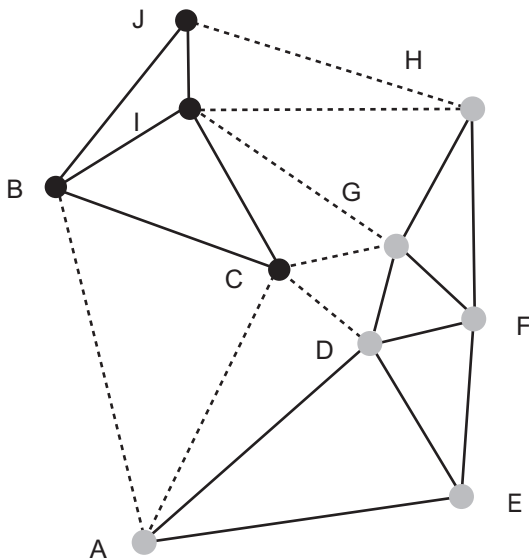


Figure 9.6 Delaunay connection links among 16 sampling locations. In a terrestrial context, e.g. forest, where only local neighbourhood effects prevail, this Delaunay tessellation network corresponds well to the ecological and environmental processes among sampling locations. However, if large-scale processes occur as well (e.g. two climatic zones indicated by black dots and grey dots), then the dashed links between sampling locations should be removed and only the solid lines should be kept.

with the *k*-means method (2 out of 5; 5 out of 10; 12 out of 20 and 26 out of 40). Here, the spatial partition based on 20 clusters divides the study area into patches that characterize the differential spatial heterogeneity of the lower part of the study area and the relatively greater spatial homogeneity of the upper part. The advantage of the hierarchical agglomerative centroid algorithm is that it is hierarchical across the partitioning when increasing the number of clusters, that is the spatial clusters found with five clusters are maintained as such when the number of clusters increases. This is not the case with the *k*-means algorithm, where at each increase in the number of clusters, the new partition does not contain the spatial clusters of the previous partition with fewer clusters. This is because the *k*-means algorithm is

an iterative procedure starting with a random assignment of locations to clusters. To reduce this problem, spatial partitioning based on a hierarchical clustering algorithm, or other algorithm, could be used as a starting assignment input for the *k*-means procedure.

- (2) Both spatial clustering and boundary detection algorithms by definition will provide either spatial clusters or boundaries even when none exist. An obvious example is the case where there is a gentle gradient across a region: the clusters or boundaries identified will not reflect true discontinuities in any ecological process but will respond most to local noise in the data. Furthermore, in some circumstances, spatial clusters may include sampling locations that have a high degree of similarity among adjacent sites, but other spatial clusters may have a high degree of dissimilarity. Finally, applying spatial constraints in clustering sampling locations may not necessarily create spatial clusters that have the strongest degree of similarity among sampling locations. For example, there could be situations where two sampling locations are not spatially adjacent but have comparable values because they are under the same climatic regime (Figure 9.6) or are influenced by the same underlying topography in terrestrial ecosystems or bathymetry in aquatic ecosystems (Figure 9.7). In such circumstances, it may be appropriate to customize the spatial constraints among the sampling locations by adding or removing links accordingly, not only to the topology of the connectivity network, but also according to physical and environmental conditions.

9.1.3 Fuzzy classification

The clear dichotomy of membership by which every location is either a member or not a member of any given group, such as presented in Section 9.1.2, may not be appropriate in all circumstances either because the quantitative data cannot be accurately classified into discrete classes (e.g. mixed forest dominated by deciduous or by coniferous species),

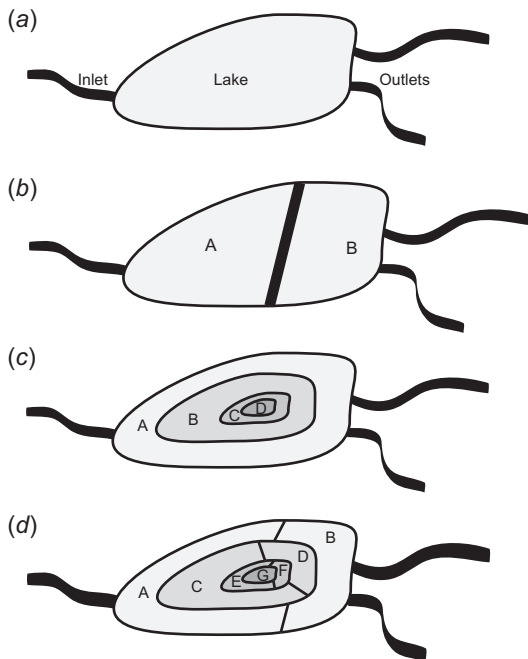


Figure 9.7 Spatial constraints in an aquatic system: (a) in shallow lakes where only local effects occur, spatial adjacency may correspond to the processes resulting in two spatial clusters A and B (b). (c) In deep lakes, bathymetry may play an important role and spatial constraints may not be appropriate. In fact, bathymetric isolines may reflect better the spatial constraints of the lakes forming four spatial clusters A, B, C and D. (d) Both spatial adjacency and bathymetry can be considered important, in which case seven spatial clusters will be formed (A, B, C, D, E, F and G).

their spatial location is uncertain or inaccurate (e.g. telemetry data), or the data measurement is only approximate (e.g. vegetation percentage cover reported in classes). Fuzzy classification and fuzzy *k*-means (see Burrough & McDonnell (1998) for mathematical details) have been suggested to be more appropriate spatial clustering methods in such cases (Jacquez *et al.* 2000). These methods are based on fuzzy set theory (Zadeh 1965) where the membership function is not a discrete dichotomy (0 or 1, an integer value) but rather a real number ranging from 0 to 1, called a 'possibility'. The possibility of being a member of a cluster is based either

on expert knowledge or on spatial location uncertainty. The membership function can take several different shapes (e.g. linear, sigmoidal, symmetric, asymmetric) defined over a range of values of a variable, called transition zones. The advantage of the fuzzy classification approach is that it may more adequately reflect ecological processes and species' responses to environmental conditions. The drawback is that it requires more knowledge about the processes and any user-defined decisions can introduce a lot of subjectivity resulting in non-optimal spatial clusters. To reduce the amount of subjectivity, the researcher can employ the fuzzy *k*-means approach (also referred to as fuzzy *c*-means, Burrough & McDonnell 1998). This method is also an iterative procedure that minimizes the within-cluster variability, but a fuzzy exponent is added to allow the overlap of clusters. When this fuzzy exponent is set to zero, it is equivalent to the *k*-means algorithm; when it is too high, all the clusters overlap. McBratney & de Grujter (1992) suggested a value of 2 as a starting point for the fuzzy exponent. Using the same tree species data, the fuzzy *k*-means (based on five classes and a fuzzy exponent of 2) produces a different spatial partition from the equivalent spatial *k*-means clustering example (Figure 9.8). Here, the five crisp spatial clusters are smaller than those obtained previously, but are surrounded by a gradient of fuzzy membership values. For illustration purposes, the possibility values were classified into five categories: 1 (1.0: 100% possibility to be part of the cluster), 2 (from 0.5 to 0.9), 3 (from 0.3 to 0.49), 4 (from 0.1 to 0.29) and 5 (0.0). Then, category 1 (100% possibility to be in a cluster) was divided into the five requested spatial clusters (A, B, C, D and E). The advantage of the fuzzy *k*-means method is that it allows determination of fuzzy boundary zones between spatial clusters.

Fuzzy set theory has been applied to detect fuzzy boundaries (among others, see Leung 1987; Edwards & Lowell 1996; Brown 1998; Burrough & McDonnell 1998; Arnot *et al.* 2004; Holden & Evans 2010). Jordan *et al.* (2008) compared two fuzzy set approaches, fuzzy classification and fuzzy boundaries, and found these methods to be complementary.

0.4	0.2	0.4	1-E	1-E	0.4
0.7	0.7	0.2	0.4	1-E	1-E
0.7	0.2	0.4	0.7	0.7	0.7
0.2	0.7	0.7	0.7	0.7	1-D
0.0	0.7	0.7	1-B	0.7	1-D
0.7	1-B	1-B	1-B	0.7	1-D
1-B	0.7	0.7	0.4	0.7	0.7
1-B	0.7	0.7	0.4	1-C	0.7
1-B	0.2	0.7	0.7	0.7	1-C
1-B	0.7	0.7	0.7	0.7	0.7
0.7	0.7	0.7	1-A	0.7	0.7
0.7	0.7	1-A	0.7	1-A	0.7
0.7	0.7	0.7	0.7	0.7	1-A
0.7	0.7	0.7	0.7	0.7	0.7

Figure 9.8 Fuzzy k -means spatial clusters of the tree abundance data of 84 sampling locations using $k = 5$. The sampling location parts of a spatial cluster have a membership possibility of 1 and are indicated by 1-A, 1-B, 1-C, 1-D and 1-E, where A, B, C, D and E signify the five spatial clusters. The other sampling locations have a membership possibility of belonging to a spatial cluster varying from 0 to 0.9999. For illustration purposes, the membership possibilities were classed into four categories: 0.7 (from 0.5 to 0.9), 0.4 (from 0.3 to 0.49), 0.2 (from 0.1 to 0.29) and 0.0 for 0. The five spatial clusters each contain very few sampling locations. In fact, most of the sampling locations almost belong to a spatial cluster (as indicate by 0.7) and illustrate the spatial extent (width, area) of the boundary zones between the spatial clusters.

9.2 Boundary delineation

Several disciplines have developed analytic tools to detect boundaries: in ecology the detection of edges, ecotones, and ecological boundaries of vegetation

types are of interest. Here we will focus on those methods that are most relevant to ecological studies (Figure 9.3).

9.2.1 Ecological boundaries

In ecology, the development of boundary detection methods has a long tradition in studies associated with ecotone delineation. Ecotones are of interest in ecology because they are at the interface between two communities or ecosystems, where the exchange of nutrients and other forms of 'information' occurs. Ecotones have distinct structural and functional properties that differ from the adjacent systems (Holland *et al.* 1991; Hansen & di Castri 1992; Cadenasso *et al.* 2003; Arnot *et al.* 2004; Hufkens *et al.* 2009). The structural properties of ecotones are directly related to the type and the strength of the underlying processes that either generate or maintain them. Thus, ecotones, or ecological boundaries, represent linear responses to steep gradients in the environmental conditions or nonlinear responses, such as thresholds, to environmental gradients (Table 9.1). Our ability to detect ecological boundaries depends therefore on the ecological process(es) under investigation (Gosz 1993; Dungan *et al.* 2002) as well as on the sampling design and analytic tools employed (Fortin & Drapeau 1995; Fortin 1997, 1999b; Fortin *et al.* 2000). Sampling designs for detecting boundaries should include sufficient sampling locations over a transect, or an area, so that not only the boundary itself but also the adjacent patches that it separates are covered.

9.2.2 Boundary properties

Before examining the geometrical properties of boundaries, we need to define some terms. The term 'edge' in the field of boundary detection and image segmentation refers to a sharp demarcation while in the field of graph theory (see Chapter 3) it refers to a link between two nodes. In image segmentation there are three major types of edges: the step edge, the roof edge and the spike edge. The step edge is the ideal case in which two well-defined and almost uniform

Table 9.1 Processes and environmental factors creating and maintaining ecological boundaries

Environment and landscape structure changes	Processes and factors creating or maintaining boundaries	Type of boundary	Ability to detect edges and the underlying processes and factors
Sharp environmental changes	Geomorphology, topography, biogeochemistry, climate	Sharp, narrow, persistent	Possible to detect abrupt changes in diversity or abundance
Gradual environmental changes	Geography, climate, species' ranges (species physiological limits), species interactions	Blurred, wide, persistent or transient	Difficult to detect changes in biomass and abundances; possible to detect compositional changes
Spatial heterogeneity within large disturbances	Fire, storm, drought, species interactions, succession	Sharp to smooth, transient	Possible to difficult depending on the intensity of the disturbance
Spatial heterogeneity within small gaps	Treefall, species interactions, succession	Blurred, transient	Difficult to detect due to qualitative and quantitative noise
No environmental changes	Species interactions, dispersal ability	Sharp, persistent	Possible to difficult depending on species interactions

patches of different types meet (e.g. forest and agriculture land), while the roof edge occurs when either or both patches are spatially autocorrelated (Philibert *et al.* 2008). The spike edge, where an abrupt change in intensity occurs only locally, is rarer in ecology than in image processing. In ecology, the term edge is mainly used to refer to the step edges of human making and their effect (edge effect; Harper *et al.* 2005). There are several equivalent terms employed to refer to step edges, such as sharp, crisp or line boundaries (Figure 9.9a, b). The opposite of sharp step edges are gradual, intermediate, fuzzy boundaries or transition zones (Figure 9.9c, d). The term boundary includes both edge (line) and gradual (zone) demarcation. Herein, we will use the term boundary to refer to both sharp and gradual edges.

Related to the notion of boundary sharpness is the boundary's width, either narrow or broad. In an ecological context, it is quite probable that the width of a boundary varies asymmetrically along the length of the boundary as well as on each side of it (Figure 9.9c, d). Hence there are locations where ecological processes are more likely to be sharper than others. This can create only localized boundaries that

do not enclose an area. Such boundaries are called 'difference' or 'open' boundaries (Figure 9.9b–d), whereas those that surround and delimit an area completely (e.g. a patch) are called 'area' or 'closed' boundaries (Figure 9.9a).

Anthropogenic boundaries tend to be straight, although not universally. Boundaries originating from natural processes, on the other hand, are often sinuous or recurving, forming a series of convex and concave shapes. The degree of straightness or sinuosity can be measured using the fractal dimension (Burrough 1981; Mandelbrot 1983). The accuracy of the fractal dimension measure, however, is directly affected by the spatial resolution of the sampling units.

Finally, all the structural and functional properties of boundaries are scale-dependent (Gosz 1993; Fortin 1999b; Csillag *et al.* 2001; Handcock & Csillag 2002; Fagan *et al.* 2003; McIntire & Fortin 2006; James *et al.* 2010, 2011). Boundary studies need to acknowledge the scale of the ecological processes being studied as well as the effects of spatial resolution, of both the sampling unit and the extent of the study area, on the accuracy of detecting boundaries (James *et al.* 2011).

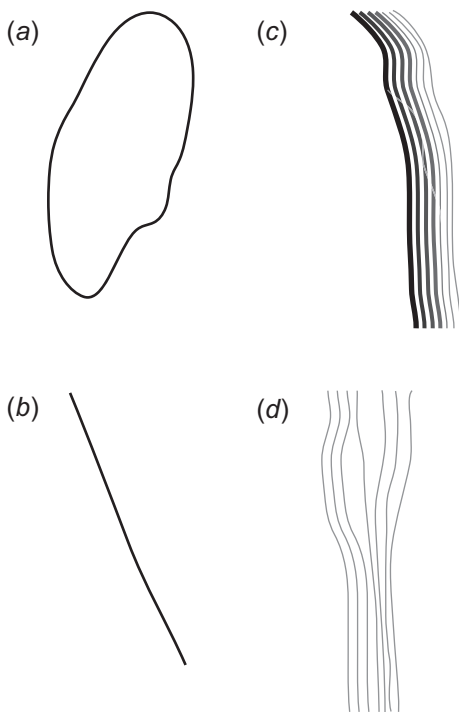


Figure 9.9 Boundary properties: sharp (crisp, step edge or line) boundaries (*a* and *b*); gradual (intermediate, fuzzy, or transition) boundaries (*c* and *d*), open (difference) boundaries (*b*, *c* and *d*) and closed (area) boundary (*a*).

9.2.3 Boundary detection and analysis for one-dimensional transect data

This section focuses on the analysis of how organisms are arranged on simple one-dimensional environmental gradients. Specifically environmental gradients considered having monotonic changes in the intensity of a single environmental factor with physical distance. The gradient is the spatially explicit version of the kinds of monotonic changes in a factor that may be detected by any ordination technique (e.g. PCA, RDA, CCA; Legendre & Legendre 2012). The concept of spatial structure is somewhat different in the context of a gradient, but it still refers to nonrandomness in space that has a certain amount of predictability. A gradient produces predictable and directional non-stationarity, and the

resulting spatial structure is in the appearance of species where they were previously absent and their disappearance as they become absent. The predictability of the spatial pattern is in how the species enter and leave along the gradient and in the relationships between the ranges and densities of the species where they are present.

The potential location of any species on the gradient is determined by its physiological responses, but the observed locations result from the interaction of physiology with ecological processes such as competition, facilitation and predation. The observed arrangement of species will determine which species will interact in the future, particularly for non-motile and sessile organisms. The organisms that occur closest together on the gradient may be the ones competing most strongly but may also be the ones with the greatest potential for positive interactions (see Bertness & Calloway 1994; Brooker *et al.* 2008).

The most familiar model of a species' response to an environmental gradient is a symmetric unimodal curve when density or activity is plotted against the intensity of the controlling factor or just the physical distance along the gradient (Jongman *et al.* 1995). These two may be different because the same physical distance along a gradient may not produce the same quantitative change in a controlling environmental factor at all locations. The familiar symmetric unimodal response curve may occur seldom in nature, with asymmetry being more common and some responses being bimodal (Austin & Austin 1980; Minchin 1989; Collins *et al.* 1993). The perceived symmetry or skewness of a unimodal response also depends on the scaling of the axis representing the environmental factor.

Organisms in their environment respond to several gradients simultaneously and combinations of gradients can produce differently shaped responses to the whole set (e.g. plants in natural vegetation; cf. Austin & Smith 1989). If there is a single known and measurable controlling factor, then a direct analysis can be made by plotting the biological response against factor intensity. If the gradient is produced

by the interactions of several variables or if the controlling factor is unknown, a more inferential approach must be used (cf. Austin 1987). Also, the rate of change in a controlling factor may vary along the length of a gradient, or organisms may respond more or less strongly to the same amount of change in the controlling factor, depending on position along the gradient. For example, the 'critical tide level hypothesis' for communities of intertidal algae suggests that there are particular levels on the shore where species replacement occurs more rapidly over small differences in height, because the response of species to changes in the duration of desiccation is much stronger at that level (Doty & Archer 1950). Similar critical levels on other kinds of environmental gradients, such as temperature or soil moisture are possible.

Species can be arranged on an environmental gradient in a variety of ways, and the arrangement can reveal much about the organization of their communities, such as critical levels in the controlling factor, or evidence about the biological interactions. For example, interspecific competition is often important on a gradient, and the inability of two competitors to coexist could result in the beginning of one species' range following immediately after the ending of another species' range; on the other hand, if species replacement allows a zone of coexistence, the density of one species decreases as the other's increases in that zone of overlap (cf. Dale 1999; Pielou 1978).

The arrangement of plant species in a community that occurs on a gradient can provide insight as to how such a community is structured (Shipley & Keddy 1987). The 'community unit' model suggests that groups of species replace each other along a gradient so that there are clusters of upper and lower boundaries (Figure 9.10). The contrasting individualistic model suggests that the species occur independently of each other, so that upper and lower boundaries occur independently and boundaries are therefore not clustered (Figure 9.10). These two models are not the only possibilities and Whittaker (1975) described two others. The four are shown in Figure 9.10 – (a) the community unit model: distinct groups of species with exclusion boundaries; (b) the individualistic

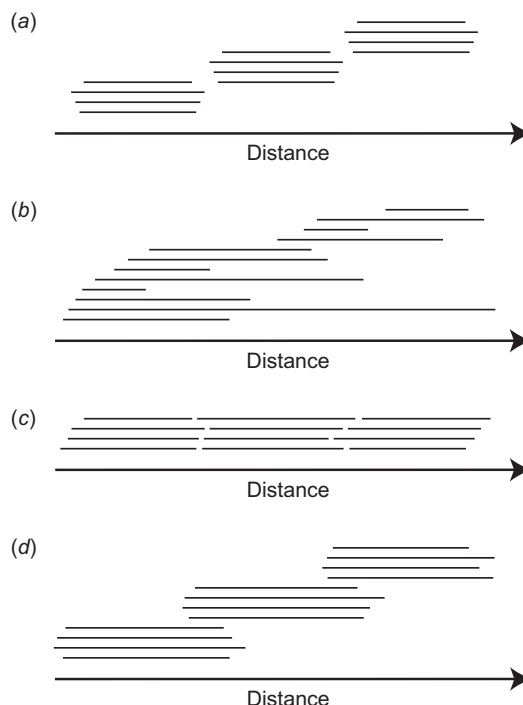


Figure 9.10 Four models of species ranges on a gradient. The presence of each species on the gradient is represented by a line: (a) the community unit model: there are zones, each consisting of a group of species that occur together and the zonal units replace each other completely over a short distance; (b) the individualistic model: the species occur more or less independently along the gradient; no groupings and no exclusion; (c) there are four sequences of species; within each sequence, one species begins where another ends: sharp exclusion boundaries between competing species but no natural groupings; and (d) there are zonal groupings of species that overlap; so the groupings of species are not exclusive.

model: no groupings and no exclusion; (c) sharp exclusion boundaries between competing species but no natural groupings; and (d) groupings of species that are not exclusive. As slight variants on these four, species replacement can be by sharp mutual exclusion or by gradual replacement with zonal overlap. Distinguishing among these possible arrangements and answering related questions can be achieved by spatial analysis in systems structured by

gradients, beginning with determining the locations of the various boundaries of interest.

9.2.3.1 Boundary detection in one dimension

For the analysis of gradients, including the detection of boundaries, both the sampling design and data type need to be considered. The obvious kinds of data are density measures and presence : absence records; the two designs are continuous transects over distance, and spaced samples such as quadrats or points.

The simplest and most effective way to detect ecological boundaries from quantitative data is to apply a moving split-window technique (Webster 1973; Johnston *et al.* 1992). This technique consists of computing the difference between two halves of the window. The window size can vary containing minimally only one sampling location per half. Various metrics can be used to measure the differences between the two adjacent window-halves (left and right halves) such as discriminant functions, Mahalanobis distances and squared Euclidean distance (Ludwig & Cornelius 1987; Brunt & Conley 1990). The squared Euclidean distance, D_{E^2} , is by far the most commonly used metric:

$$D_{E^2}(x_1, x_2) = \sum_{i=1}^p (z_{1i} - z_{2i})^2, \quad (9.2)$$

where x_1 and x_2 are the two sampling locations to compare and z_{1i} and z_{2i} are the values of the p variables at these two locations. The window is then slid along the entire transect, one sampling location at a time, so that all adjacent sampling locations can be compared. In the example illustrated in Figure 9.11, each half contains the data from one sampling location and resulting measures are located between the sampling locations for a total of $n - 1$ difference values. Sharp boundaries occur where high and narrow peaks identify the location of ecological boundaries, whereas gradual boundaries occur where peaks are low and wide. By computing differences based on adjacency, the moving split-window is in essence a local boundary detector. The drawback of all local boundary detectors is that they are

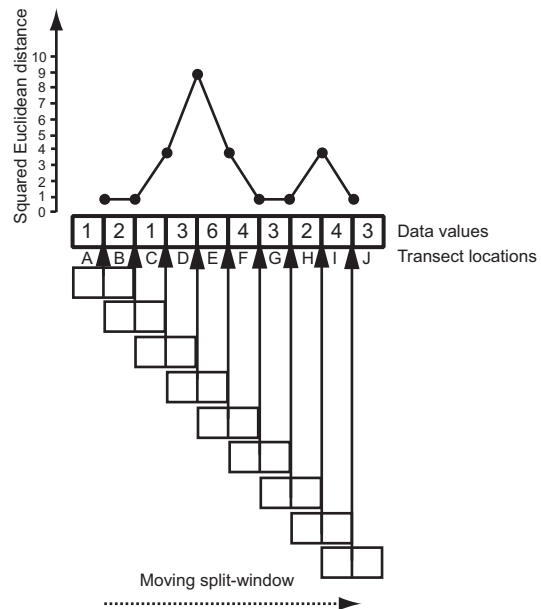


Figure 9.11 Moving split-window along a transect of ten contiguous sampling locations. The moving split-window size is two sampling units (one sampling unit in each half). The squared Euclidean distance computed for each pair of sampling units resulting in nine values where the strongest peak (i.e. boundary) is between the sampling locations D and E and the second, weaker peak between sampling locations H and I.

sensitive to local noise in the data. To minimize the undesirable effects of local noise, computation of the differences can be performed using windows of increasing sizes. The results can then be drawn on the same plot where peaks corresponding to ecologically meaningful boundaries will persist while peaks due to local noise will be smoothed out. Ecological boundaries will produce peaks at the same locations. The similarity to analysis with a Haar wavelet is obvious (Dale *et al.* 2002; James *et al.* 2011; James & Fortin 2012).

Comparable methods are available for presence : absence data collected at contiguous sampling locations. Basically, the observed number of species present at a given location is compared against a random distribution derived from a Monte Carlo procedure: Dale's method (1986, 1988) computes

the amount of spatial overlap at each location, while the technique of McCoy *et al.* (1986) is based on the probabilistic similarity between pairs of sampling locations. A different approach can be used in which the presences and absences of the individual species are initially dealt with as a separate source of data for analysis, usually summarized as the species' range on the gradient, with its end-points defined by the first and last occurrences of the species. There are some interesting questions about the meaning and importance of absences within any one species' range, but there are a number of advantages to using this kind of data to study the boundaries of species in one dimension, as we will now describe.

9.2.3.2 Evaluating boundaries in continuous presence : absence data

Given continuous records of presence : absence data, each species range is known and is defined directly by its first and last occurrence on the explicit gradient. The mathematical techniques of combinatorics provide a useful approach to the spatial analysis of such simple data.

This simple approach ignores species abundances and represents the range of each species on the gradient as a line segment joining the uppermost and lowermost occurrences. The whole set of species on the gradient is therefore represented by a 'sheaf' of line segments, the positions and lengths of which correspond to the species' ranges on the gradient. Given data in this format, there are a number of approaches to detect particular features of the data. As presented in Section 9.2.2, there are at least four models to consider in describing species' ranges, based on Whittaker (1975) as in Figure 9.10:

- (1) distinct groups of species with exclusion boundaries (the community unit model);
- (2) no groupings and no exclusion (the individualistic model);
- (3) sharp exclusion boundaries between competing species but no natural groupings;
- (4) groupings of species that are not exclusive.

These methods will be illustrated using the ranges of seaweed species on rocky intertidal shores on which

there is an indirect environmental gradient of the time of emergence from seawater each day, which acts mainly through desiccation and temperature effects. The data included are from three sites in Yarmouth County, Nova Scotia (approximately 43° 40' N, 66° W). Each site was sampled at several stations using three to seven line transects from above the high tide level to the upper subtidal (about 3.6 m elevation). The shores are gently sloping and the most common species were *Ascophyllum nodosum*, *Fucus spiralis*, *Fucus vesiculosus*, *Fucus serratus*, *Chondrus crispus*, and *Gigartina stellata*. The transects recorded the species' linear positions as they intersected the edge of a measuring tape and thus, the positions of the upper and lower boundaries of each species were determined. There were 29 transects in all (for details see Dale 1999). To distinguish among the various models of how the species ranges are arranged on the one-dimensional gradient, we can examine the overlap of ranges, the intermingling of upper and lower boundaries, the contiguity of ranges, and the clustering of boundaries. The consistency of the order of boundaries at different parts of the shore can be measured by concordance statistics.

Overlap of ranges

One approach to the analysis of species ranges on a gradient was originated by Pielou (1977b). The overlap of ranges is evaluated by counting the numbers of pairs of species in three classes designated by the variable λ : no overlap, $\lambda = 0$; partial overlap of the pair of ranges, $\lambda = 1$; one range completely overlaps the other, $\lambda = 2$ (Figure 9.12). The numbers in the three classes are compared with the expected values based on one of several null hypotheses (Pielou 1977b, 1978). Those numbers are summarized by the overlap vector $\mathbf{L} = (\omega_0, \omega_1, \omega_2)$, in which ω_t is the number of pairs of lines for which $\lambda = t$. For n species, $\omega_0 + \omega_1 + \omega_2 = n(n-1)/2 = k$. The simplest null hypothesis, H_0 , is that the order of the $2n$ events, n beginnings and n endings, is fully random subject to the constraint that each ending follows its own beginning. On this null hypothesis (Pielou 1977b; Dale 1979):

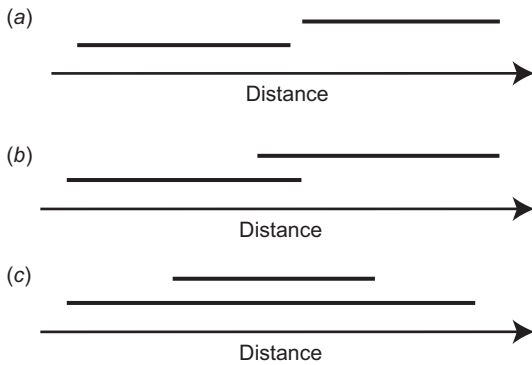


Figure 9.12 Definition of λ for any pair of species ranges: (a) $\lambda = 0$ where there is no overlap; (b) $\lambda = 1$ where there is partial overlap; and (c) $\lambda = 2$ where there is complete overlap of one range by the other.

$$E(\mathbf{L} | H_0) = k(1, 1, 1)/3 \quad (9.3)$$

and

$$\text{Var}(\mathbf{L} | H_0) = 2k(2n + 1, n + 3, n + 3)/45. \quad (9.4)$$

For $n = 12$ species, $E(\mathbf{L} | H_0) = (22, 22, 22)$ and $\text{Var}(\mathbf{L} | H_0) = (73.3, 44, 44)$. If the distributions of the ω_i can be assumed to converge to the normal distribution, the 95% confidence limits for \mathbf{L} are (5, 9, 9) and (39, 35, 35), but these must be used with caution for drawing conclusions about departures from randomness because the three values in \mathbf{L} are not independent. We could, however, choose one of the three and focus on evaluating its departure from expected values.

On the other hand, if we have a set of many transects, we can examine the signs of $\mathbf{L} - E(\mathbf{L} | H_0)$ for trends. In the 29 transects from the three Nova Scotia sites, there was a tendency for $\mathbf{L} - E(\mathbf{L} | H_0)$ to be of the form (+, -, -), suggesting an overabundance of non-overlapping pairs.

H_0 is useful for evaluating \mathbf{L} , but to examine the actual lengths of overlap of species' ranges, a second null hypothesis, H_d , is required. This hypothesis assumes that the length of each species' range measured along the gradient is fixed, but that the boundaries are otherwise placed randomly and independently. Given the range of length a and a total gradient length

w , the position of the upper boundary will follow a rectangular probability distribution running from 0 to $(w - a)$. For any pair of species' ranges, let a be the longer and b the shorter. If $a + b > w$ then $\lambda > 0$, so those pairs need to be treated separately. Let A be that set of pairs and let B contain all other pairs. Then

$$E(\omega_0 | H_d) = \sum_A \frac{(w - a - b)^2}{(w - a)(w - b)}, \quad (9.5)$$

$$E(\omega_1 | H_d) = \sum_A \frac{b(2w - 2a - b)}{(w - a)(w - b)} + \sum_B \frac{(w - a)}{(w - b)}, \text{ and} \quad (9.6)$$

$$E(\omega_2 | H_d) = \sum_A \frac{(a - b)}{(w - b)} + \sum_B \frac{(a - b)}{(w - b)}. \quad (9.7)$$

The overlap vectors for the seaweed data were compared with the expected values based on H_d . Again, the ω_0 values tended to be larger than expected, so that $\mathbf{L} - E(\mathbf{L} | H_d)$ tended to be of the form (+, -, -). The fact that this tendency was found for H_d as well as for H_0 means that fewer pairs of ranges overlapped than expected, even when the lengths of the ranges were considered.

In some cases, the study of patterns of overlap can be augmented by evaluating related characteristics such as the sizes of gaps between non-overlapping ranges and the sizes of partial overlaps where those occur. Dale (1999) provided a summary of how such evaluations can be made using either measured distances or using the number of boundaries as a measure of length.

Intermingling of upper and lower boundaries

The extent to which the two kinds of events, upper and lower boundaries, are intermingled along the gradient is another characteristic that may be of ecological interest. To measure this intermingling, we can redefine ω_0 , by setting q_i as the number of lower boundaries that are above the i th upper boundary. Then,

$$\omega_0 = \sum q_i. \quad (9.8)$$

This variable counts non-overlapping pairs, but also provides a measure of the intermingling of upper and

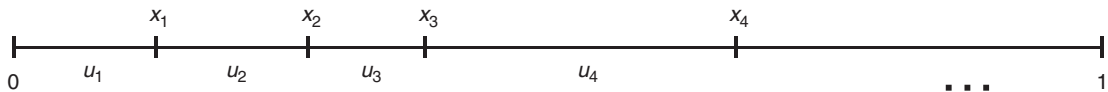


Figure 9.13 Random numbers in the interval 0 to 1, x_1, x_2, \dots, x_m , break the interval into $m+1$ segments, u_1, u_2, \dots, u_{m+1} .

lower boundaries. Where X is an upper boundary, and o is a lower boundary, the sequence $XXXXoooo$ is an example in which the two kinds are fully separated and $\omega_0 = 0$; in contrast, the sequence $XoXoXoXo$ has the two kinds highly intermingled and $\omega_0 = 6$. We commented earlier that, because the three ω_t are not independent for different values of t , we cannot make valid tests of all three, but we can legitimately test one of them, ω_0 . The critical values for ω_0 can be derived from the frequency distributions or from the normal approximation, and the values are summarized in Dale (1999). When we applied this test to the Nova Scotia seaweed data, ω_0 was greater than expected in 26 of the 29 transects, but only 11 were significant at the 5% level. These results confirm a tendency for greater intermingling of upper and lower boundaries, indicating that species turnover along the gradient is greater than expected.

Clumping of boundaries

Another spatial characteristic of a sheaf of species' ranges that is often of ecological interest is the extent to which the species' boundaries are clumped together or widely spaced along the gradient. For example, this characteristic can help to distinguish among the different arrangements of species on a gradient: the clumping of boundaries is predicted by the community unit model described above. It could also be a characteristic involved in testing hypotheses like the critical tide level hypothesis (Doty & Archer 1950), whereby the boundaries tend to be clumped where the gradient's effects are most intense.

To evaluate clumping, the length of the gradient can be standardized to 1, with 0 at the first boundary and 1 at the last. The other boundaries are then points in the unit interval, x_1, x_2, \dots, x_m , which break the interval into $m+1$ parts, u_1, u_2, \dots, u_{m+1} (Figure 9.13). Where there are n species and the whole gradient is considered, $m = 2n - 2$, but m may be less if sampling does not include all boundaries. If the boundaries are clumped, there will

be many small segments (within clumps) and a few large segments (separating the clumps), and so a first step is to measure the variability of the u s.

For this purpose, the measure

$$W_m = \sum_{i=1}^{m+1} u_i^2 \quad (9.9)$$

has been introduced under a variety of names (for example, Darling 1953). If the x_i s are randomly and independently placed in the unit interval, each governed by a rectangular distribution on $(0, 1)$, the mean and variance of the distribution of W_m are

$$E(W_m) = 2/(m+2) \text{ and} \quad (9.10)$$

$$V(W_m) = 4m/[(m+2)^2(m+3)(m+4)]. \quad (9.11)$$

The distribution is asymptotically normal with increasing m , but convergence is slow (Moran 1947). It is therefore impractical to derive critical values from that approximation but a Monte Carlo approach can be used instead. The statistic W_m essentially measures the variability of the unit interval's internal segment lengths, and so it is sensitive to boundaries occurring as close together as pairs; but it does not detect clumps consisting of more than two boundaries. That characteristic requires a second statistic to measure the serial autocorrelation of adjacent segment sizes:

$$h_m = \sum_{i=1}^m u_i u_{i+1}. \quad (9.12)$$

Based on the same null hypothesis, its mean and variance are (Dale 1988):

$$E(h_m) = m/[(m+1)(m+2)] \text{ and} \quad (9.13)$$

$$V(h_m) = (m^3 + 3m^2 + 4m - 4)/[(m+1)^2(m+2)^2(m+3)(m+4)]. \quad (9.14)$$

The distribution of h_m seems to approach the normal distribution more rapidly than that of W_m .

To illustrate the performance of these two indices, consider the sequence of intervals 0.001, 0.001, 0.001, 0.001, 0.001, 0.147, 0.15, 0.45, 0.25; these data give $W_8 = 0.309$ and $h_8 = 0.202$, which are both significantly high. When the data are rearranged with alternating high and low values, 0.001, 0.147, 0.001, 0.15, 0.001, 0.45, 0.001, 0.25, 0.001, W_m is unchanged but h_m declines to $h_8 = 0.002$, which is significantly low. Almost all combinations of test results for the two statistics seem possible, except for W_m being significantly low and h_m significantly high.

When the boundaries are clumped, it may be useful to identify where the boundaries are most clumped together, perhaps indicating critical levels of the controlling factor. The recommended procedure is to identify the sections of the gradient where the observed concentrations of boundaries have the lowest probabilities based on the null hypothesis of independent random placement. The details of how this can be done are given in Dale (1999), based on Dale (1988). As in the identification of boundaries in two dimensions using wombling (Fortin 1994; Section 9.2.4), the process initially produces candidate boundary clumps, all those with low probability, followed by determining which are the 'best' of these, as indicated by the lowest associated probability. By default, the patches between the best boundary clumps are those with the most distinct or well-distinguished species composition.

9.2.3.3 Evaluation of boundaries in contiguous quadrat data

Many studies of the pattern of species on environmental gradients have used contiguous or spaced quadrats and recorded density or presence : absence in them (Wulff & Webb 1969; Hoagland & Collins 1997). Quadrat data can be used for many of the kinds of analyses described above, such as overlap, gap size, intermingling of boundary types, and clustering of boundaries. If the quadrats are small enough that there is never more than one boundary in a quadrat, then the methods described above for continuous

ranges can be used directly, with quadrat position in the sequence being the equivalent of distance along the transect. The problem comes when the quadrats are larger producing ties in the ranking of boundary order. These ties obviously represent a loss of information. If the relationships among the ranges and boundaries of species are of interest and quadrats contain more than one boundary, the quadrats are too small and the scale of sampling does not match the scale of the pattern.

In a transect of contiguous quadrats on an environmental gradient, provided that the length of the transect is sufficient, some quadrats will contain the upper boundaries and some will contain the lower boundaries of the species of plants in the area. There are a number of questions that can be asked about such data, either collectively (such as: are the upper boundaries clumped?) or at the level of the individual species (such as: is the range of species A along the gradient greater in the absence of competition?). Clearly, no single measure or test statistic will tell us everything we want to know, and we should be prepared to use several complementary approaches, even if they are not totally independent. The choice and effectiveness of methods may depend on the relationship between the number of species and the number of quadrats. The interpretation of a given number of quadrats containing no boundaries will be different if there are 20 quadrats and 200 species than if there are 200 quadrats and 20 species.

The analysis of quadrat data will depend in part on the null model under consideration, and there are a variety of ways of constructing null models for transects of contiguous quadrats along an environmental gradient. The usefulness of any null model as the basis for statistical tests will depend on the number of replicate transects, the number of quadrats, numbers of species, the strength of the gradient, and so on. We can provide a partial list of possible approaches and the characteristics that might be addressed.

- (1) Null models based on observed presences and absences in the quadrats:
 - (a) single species: length of range; range continuity

- (b) two species: coincidence or repulsion
- (c) many species: species combinations as 2^k records (Dale 1999, figure 5.8).
- (2) Null models based on observed ranges (the sliding stick approach):
 - (a) two species: overlap and spacing
 - (b) many species: overlap characteristics of the 'sheaf' of ranges.
- (3) Null models based on the positions of boundaries:
 - (a) upper boundaries: clumping, spacing, evenness, etc.
 - (b) lower boundaries: clumping, spacing, evenness, etc.
 - (c) comparison of (a) and (b)
 - (d) upper and lower: contiguities, intermingling, etc.
- (4) Null models based on quantitative measures in each quadrat:
 - (a) single species: shape of distribution (unimodal, bimodal, skewed); autocorrelation;
 - (b) two species: correlation, etc.
 - (c) many species: distribution of modes, nestedness, etc.

Some of these approaches have already been discussed and others will be described in greater detail below, although we will not attempt to deal thoroughly with them all.

9.2.3.4 Evaluating boundary patterns in quadrats with presence : absence

Consider a transect of Q contiguous quadrats, with k species, giving k upper and k lower boundaries. Often the two different kinds of boundary will be analysed separately. Treating one of them, let q be the number of quadrats that contain at least one such boundary, with $e = Q - q$ quadrats that contain none. The first test is to determine whether one of q or e is unusually large or unusually small.

The probability, given complete randomness that a particular quadrat is empty is $(1 - 1/Q)^k$, and so $E(e) = Q(1 - 1/Q)^k$. Then, with O and E being the observed and expected values, a standardized residual (Pearson's or Freeman-Tukey) can be compared with the standard normal distribution. For example, with $Q = 10$ and

$k = 12$, the expected number of quadrats with no boundary is $10(0.9^{12}) = 2.8$. If seven quadrats have no boundary, Freeman-Tukey residual is $z(7) = \sqrt{O} + \sqrt{O+1} - \sqrt{4E+1} = \sqrt{7} + \sqrt{8} - \sqrt{12.2} = 1.98$, indicating a significantly large number. Under the same conditions, if all quadrats had at least one boundary, then the residual is $z(0) = \sqrt{0} + \sqrt{1} - \sqrt{12.2} = -2.46$, suggesting a significantly low number.

Where the positions of the boundaries are not known, the tests for the clustering of species boundaries described above will not work and a different approach is needed to detect clustering of upslope or downslope boundaries (cf. Pielou 1975a, 1979; Shipley & Keddy 1987).

There are Q quadrats, of which q contain at least one of the K boundaries being considered. Pielou's approach was to calculate p_q :

$$p_q = \binom{Q}{q} \binom{K-1}{q-1} \div \binom{Q+K-1}{K}. \quad (9.15)$$

When exactly z quadrats contain boundaries, calculating the probability, P_z , can test whether z is sufficiently small by comparing it with the chosen significance level:

$$P_z = \sum_{q=1}^z p_q. \quad (9.16)$$

Another approach is to convert the numbers of all boundary counts to proportions, p_i being the proportion of all boundaries that occur in the i th quadrat, and then examine the evenness of the non-zero values:

$$\xi = \frac{1 - \sum_{i=1}^Q p_i^2}{1 - 1/s}. \quad (9.17)$$

For example, if only three quadrats contain boundaries, and the numbers contained are 4, 8, and 4, the evenness is $\xi = 0.9375$; if the values are 1, 2 and 13, $\xi = 0.48$.

The evenness measure is similar to many used in the literature, such as Morisita's index of clumping or the variance-to-mean ratio (Dale *et al.* 2002), in that it is not spatial. A transect of 12 quadrats with the numbers of boundaries being (0, 0, 4, 0, 0, 0, 8, 0, 0, 0, 4, 0)

produces the same evenness measure as (0, 0, 0, 0, 4, 8, 4, 0, 0, 0, 0, 0). In some cases, we may be interested in distinguishing between these two. To include the relative positions of the values, we can use the sum of the products of adjacent proportions:

$$\eta = \sum_{i=1}^{Q-1} p_i p_{i+1}. \quad (9.18)$$

In the first example above, $\eta = 0$, but in the second $\eta = 0.25$. In fact, we can calculate η_{\max} for any set of quadrat boundary counts, and then look at $\omega = \eta/\eta_{\max}$. In the first example $\omega = 0$, of course, but in the second $\omega = 1.0$. If the boundaries are rearranged slightly to give (0, 0, 0, 0, 0, 8, 4, 4, 0, 0, 0, 0), $\eta = 0.1875$ and $\omega = 0.75$.

If we have available the data from a set of transects, rather than from a single transect, there are more ways of analysing the information. Underwood (1978a, b) showed that under those circumstances, the expected value of q is

$$E(q) = Q[1 - (1 - 1/Q)^K]. \quad (9.19)$$

For each transect of the set, the deviation of the observed value from the expected is calculated, and then the mean and sample variance of the deviations are calculated and the standard t test is used to see whether the mean is significantly different from zero. This approach will have fewer applications because it requires several transects although its resolving power will increase if more transects are available. There should also be some concern, however, about the effects of positive spatial autocorrelation in the data which will reduce the independence among the transects, and will usually result in more apparently significant results than the data actually justify.

9.2.3.5 Evaluating boundaries in density data

We have been discussing methods for analysing presence : absence data, recorded in a continuous fashion, so that the end-points of the species' ranges are known. In considering species' ranges, we represented them as solid lines, although a more realistic representation of the species occurrence would be an irregularly broken line with many small gaps. In the same

way, an accurate continuous record of density (not just presence) might be extremely irregular and would then have to be smoothed to produce a curve. The use of such density data (original or smoothed), in the broad area of multivariate analysis, include direct gradient analysis, niche overlap measurement, and so on. Those topics are covered with varying degrees of detail and sophistication in other places (Legendre & Legendre 2012; among others), and we will not repeat that coverage. Many of the kinds of analysis already presented in this chapter can be used with such data.

Gradients can be spatially continuous or spatially discontinuous (Keddy 1991). In the first case, analysis may be easy and straightforward, but, in the second, the gradient will have to be (re)constructed by the researcher. Perhaps the most important feature of density data is that it allows us a quantitative evaluation of a species' response to the environmental gradient within its range. The usual model of a species' response is the Gaussian or bell-shaped curve but in general, few species are likely to have this idealised response, instead being either asymmetric, bimodal, or irregular (Austin & Austin 1980; Minchin 1989; Austin *et al.* 1994; Jongman *et al.* 1995; Legendre & Legendre 2012).

Density data also allow us to look at the among-species pattern along a gradient, by examining the relative positions of the density modes of the species. For instance, Minchin (1989) examined some of the propositions of Gauch & Whittaker (1972) concerning the organization of species' responses by testing whether the modes of the major species were evenly distributed along the gradient, perhaps because of competition and resource partitioning, and whether the modes of the minor species were randomly distributed. For data from Tasmanian montane vegetation, they found that the modes of the major species were in fact randomly distributed.

Spatial structure on environmental gradients is an important aspect of the spatial organization in ecological systems. This kind of spatial pattern includes characteristics such as the upper and lower boundaries of species, the ranges of their presence, and the way in which the densities of individual species respond to the gradient. All these characteristics can be used to help ecologists to generate ideas and to test hypotheses about how the systems are assembled and how

they function. There is more research to be done to understand this kind of spatial pattern and the processes that give rise to it, particularly as related to the detection of boundaries in multivariate data and the delimitation of multivariate (multispecies) patches. One-dimensional transect data allow only detection of the sharpness and width of boundaries, and the determination of other properties of boundaries requires two-dimensional area data. The next section will present boundary detection methods for such two-dimensional data.

9.2.4 Boundary detection based on two-dimensional data

In two dimensions, boundaries can be detected based either on categorical information or on continuous quantitative data. For quantitative data, one operational definition of a boundary is the location in space where the change of intensity in a set of variables is the greatest (Burrough 1986; Fortin 1994). For qualitative data, a boundary is the location in space where species or category turnover is the highest.

9.2.4.1 Lattice data

Two-dimensional data can be derived from a complete regular lattice of sample locations or from an irregular sampling of the area. We will refer to the former as lattice data where the spacing between any adjacent sampling units is constant. In a square lattice, each sampling unit has four adjacent sampling units, directly north, south, east and west, forming a checkerboard pattern. Other regular lattice arrangements are possible such as hexagonal. The main advantage of using two-dimensional area data over one-dimensional transect data is that all the boundary features can be estimated, including sharpness, width, shape, sinuosity, and so on.

As for the one-dimensional boundary detection methods, most boundary detectors for two-dimensional area data compute some difference among locally neighbouring locations by either moving windows or kernel filters. The difference between the two seems subtle, but it is not.

Moving windows compute a metric based on the values from adjacent sampling locations forming a square (e.g. a window size of 2×2 sampling locations) that quantifies the degree of difference among the four values (see the lattice-wombling section below). After sliding the window over the entire lattice of sampling points, the resulting number of computed metrics is less than the original number of sampling locations (Figure 9.14a). Because four sampling locations are needed to compute a difference, lattice data having n rows and m columns will produce $n - 1 \times m - 1$ rates of change. The shape of the moving window can vary and, for example, the difference can be based on three adjacent sampling locations forming a triangle instead of a square (see triangulation-wombling described below). In this section, we will present only one of these algorithms: the Womble's first partial derivative algorithm (Womble 1951).

Kernel filters operate differently. Kernels are usually squares of various sizes (e.g. 3×3 , 5×5 , 7×7 , etc.), where each cell of the kernel contains a value that is multiplied with the value at the correspondent location of the original lattice and where the resulting summation of all these products is assigned to the centre cell. This procedure is called a convolution in GIS and remote sensing applications. As for the window approaches, the kernel filter is then slid over the entire area but unlike the former, the kernel filters produce a new value for each cell of the lattice, producing as many scores as the original number of sampling locations: $n_{\text{rows}} \times m_{\text{columns}}$ (see Figure 9.14b). There are several filters (mathematical operators or templates) available, with different abilities to enhance the edges of an object (Pitas 2000; Shih 2009).

Lattice-wombling: with quantitative lattice data, the difference (hereafter called rate of change) in values among the four adjacent sampling locations forming a square (i.e. a 2×2 square window) can be estimated by computing the first partial derivative of a variable in the x and y spatial direction (Womble 1951):

$$m = \sqrt{\left[\frac{\partial f(x, y)}{\partial x}\right]^2 + \left[\frac{\partial f(x, y)}{\partial y}\right]^2}, \quad (9.20)$$

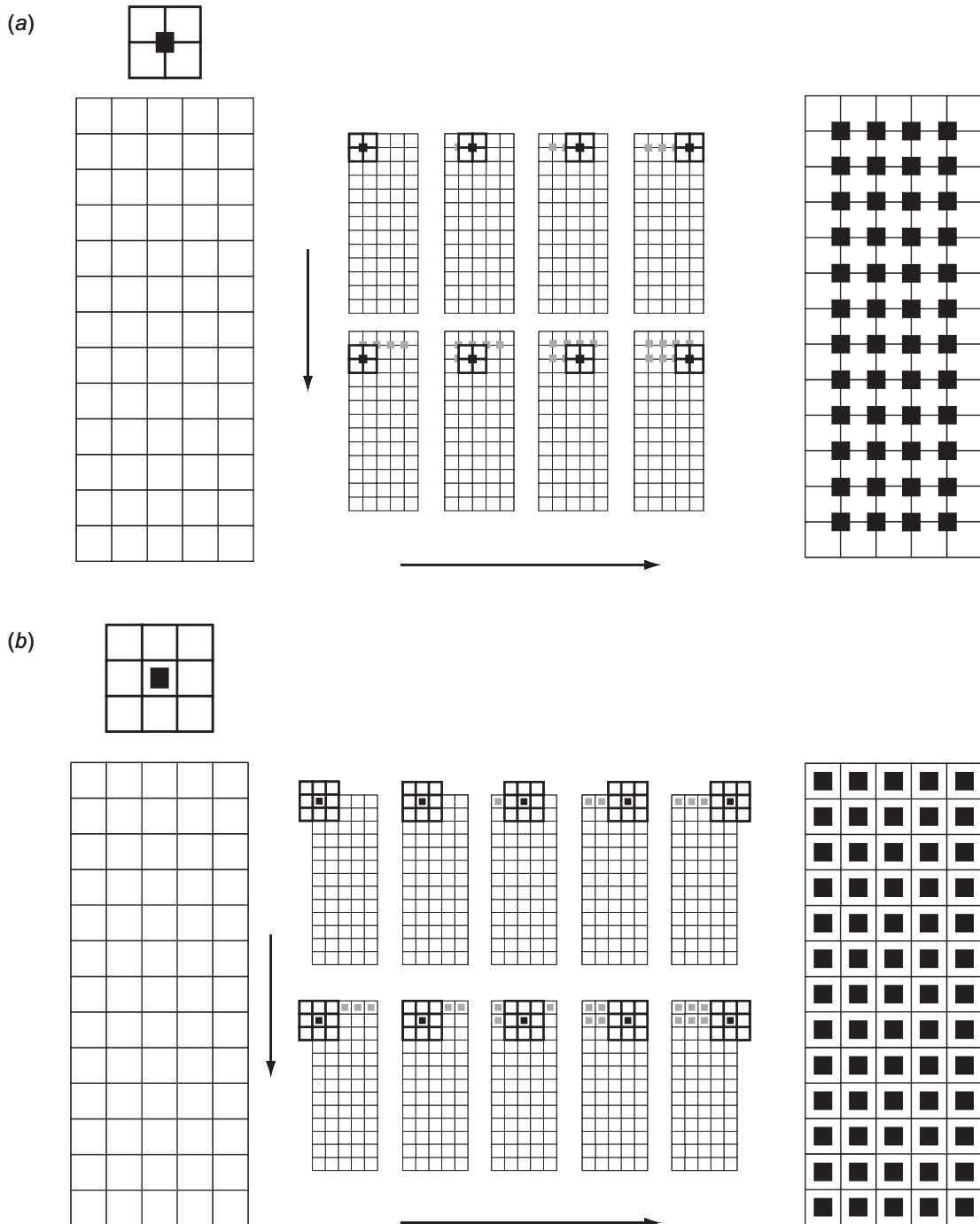


Figure 9.14 Difference measures computed by window (a) and kernel filters (b) to detect a boundary. The window or the kernel, respectively, is slid one sampling unit at a time in the x and then in the y direction over the entire study area, and the difference at the centroid location of the window (the square in (a)) or at the central cell of the kernel (the square in (b)) computed. By doing so, there are fewer difference values computed with the window approach than in the original data ($n_{\text{rows}} - 1 \times m_{\text{columns}} - 1$) but not in the kernel approach where there are the same number of difference values as number of sampling locations.

where $f(x, y)$ is a bilinear function, in the x and y spatial direction, of values z_i at the four sampling locations ($i = 1, 2, 3$ and 4):

$$f(x, y) = z_1(1-x)(1-y) + z_2x(1-y) + z_3xy + z_4(1-x)y. \quad (9.21)$$

This formulation assumes that the distance between these four sampling locations is small. For convenience, the actual x and y coordinates are scaled to range from 0 to 1. The value of the rate of change, m , is computed for the centroid of a square window. Subsequently, the square window is slid over the entire lattice by shifting one sampling location at a time. In a multivariate context, the difference among the four adjacent sampling locations is the average, \bar{m} , of the absolute values of the first derivatives of each variable, m . When there is only one variable, the detected boundaries reflect high difference in the values of that variable; when several variables are available, both the amount of species turnover as well as their difference in values affect the location of the boundaries.

Given that the rate of change is computed according to spatial direction, it is also possible to compute the orientation, angle, of the change (Barbujani *et al.* 1989):

$$\theta = \tan^{-1} \left[\frac{\left(\frac{\partial f}{\partial x} \right)}{\left(\frac{\partial f}{\partial y} \right)} \right] + \Delta, \quad (9.22)$$

where

$$\Delta = \begin{cases} 0^\circ, & \text{if } \left(\frac{\partial f}{\partial x} \right) \geq 0, \\ 180^\circ, & \text{otherwise.} \end{cases} \quad (9.23)$$

The orientation of the gradient is established by first doubling the angles to avoid slopes of opposite direction cancelling each other, then averaging and halving the result. When the highest rate of change in one variable occurs in a north-south direction and that in another variable in a south-north direction, we do not want these two directions to cancel but to reinforce this axis.

In essence, the magnitude of the rate of change, m , is the slope of the plane that can be fitted to the values of the variables at the four adjacent sampling locations (Figure 9.15). Boundaries, defined as the spatial location where high rates of change occur, correspond to

steep gradients among the four values of a variable. Weak differences among adjacent values will result in low (close to zero) values for rates of change. Such adjacent locations of low rates of change can be considered as a spatial homogeneous cluster: a patch. The major problem is to decide the threshold value of rate of change for boundary detection (Figure 9.15). When an arbitrary threshold is used, say the highest 10th percentile (Fortin 1994, 1997, 1999b), the rates of change identify what can be called 'potential' or 'candidate' boundary elements. Subsequently boundary properties (length, width, shape, etc.) can be measured in terms of spatially connected candidate boundary elements using the boundary statistics (Section 9.3). The selection of the threshold depends on the context (strength of the boundaries and their number) and the number of sampling locations (Fortin 1999b).

As an example, lattice-wombling rates of change and their orientation were computed for a set of abundance data of 26 tree species (Fortin 1992, see Figure 9.16). The values of the rates of change were ranked in decreasing order and classified into 10 categories each being a 10th percentile: the highest percentile is indicated by 1, and the lowest by 10. Here, the number of candidate boundary elements at the 10% threshold is 7 out of 65 rates of change ($14 - 1 \times 6 - 1 = 65$ rates of change). There are cases, however, where at the cut-off rank between two percentiles, the rate of change value is exactly the same as the highest percentile. In such circumstances, in order to avoid bias in the selection of one rate of change location against another, it is recommended to continue to rank all rates of change that have the same values with the same percentile class and to include them all as candidate boundary elements. Here we selected the arbitrary threshold to be 10% (indicated by 1) to designate the candidate boundary elements. The candidate boundary elements that are adjacent to one another are linked in Figure 9.16a. It is found that there are candidate boundary elements in the lower part of the study area as well as in the middle. At a threshold of 10%, the candidate boundary elements are 'difference/open' boundaries that demarcate the strongest local boundaries. Looking at the subsequent highest rates of change (say 2, 3 and 4 ranked values in Figure 9.16a), these locations coincide with the demarcation among

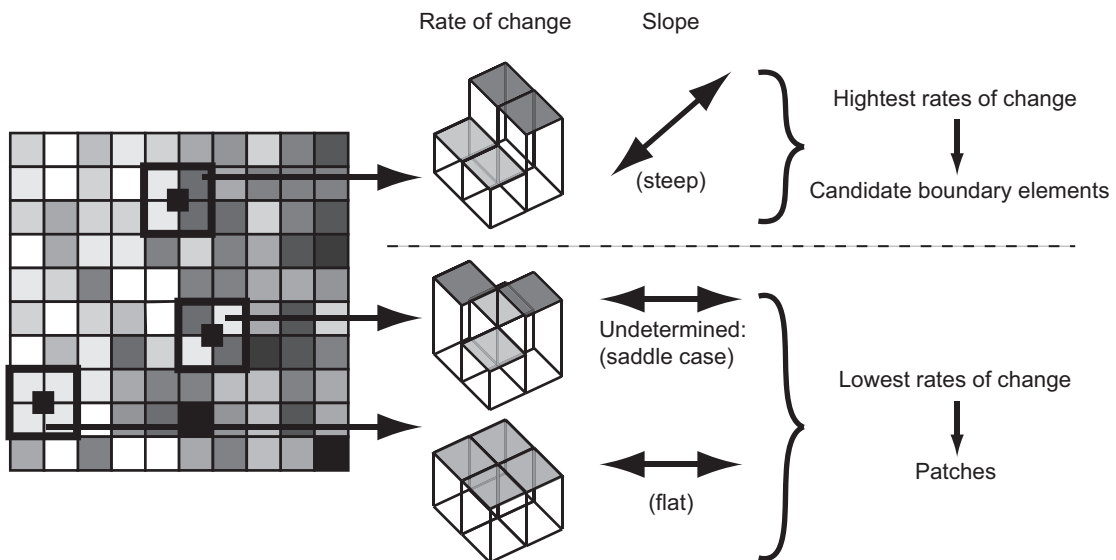


Figure 9.15 Lattice-wombling algorithm. Rates of change based on lattice-wombling are in essence the slope of the plane that fits the four values of the variable at the sampling locations. The orientation of the slope could also be useful in some studies. When the rates of change are ranked in decreasing order of magnitude (highest values of the slope), the candidate boundary elements are determined using an arbitrary threshold. When the rates of change are very low, close to zero, the sampling locations are most likely part of a patch.

the spatial clusters based on the *k*-means algorithm with 20 clusters (Figure 9.5). Spatial clustering and boundary detection can be used as complementary methods to highlight different particularities of a study area: that is complete spatial partitioning (spatial clusters) and the spatial location and properties of the boundaries (width, shape, sinuosity) between the patches (Fortin & Drapeau 1995).

As mentioned above, rates of change measure the magnitude of the slope of the gradient among adjacent sampling locations, demarcating boundary elements at the steepest part of the gradient (Figure 9.15). To obtain a better indication of a boundary's width and where it ends, second derivatives can be computed to identify the inflection point location corresponding to the limit of a boundary (Figure 9.17). Again, selecting only the highest 10% of values of second derivatives (closed circles in Figure 9.16a), their location indicates where the boundaries end. The orientation associated with the rates of change is not very informative in the present case (Figure 9.16b). Indeed, this woodlot has

several local gaps that make orientation of the rates of change uninteresting. In studies dealing with large-scale processes, as in Barbuji *et al.* (1989) where they investigated the migration path of human populations in Europe, the orientation of the rates of change may provide interesting insights.

The significance of each candidate boundary element cannot be tested using a complete spatial randomization procedure. The reason is that complete spatial randomness tests assume that each datum is independent. This is not the case in areas where patches and boundaries are suspected to occur because, within the patch and around the boundary zone, nearby sampling locations are more likely to have similar values (Fagan *et al.* 2003). When a complete randomization procedure is applied, the value of one patch can be placed next to that of another patch, creating a higher rate of change than in the observed data. Complete randomization is therefore much too conservative to test the significance of candidate boundary elements (Oden *et al.* 1993). A restricted randomization test,

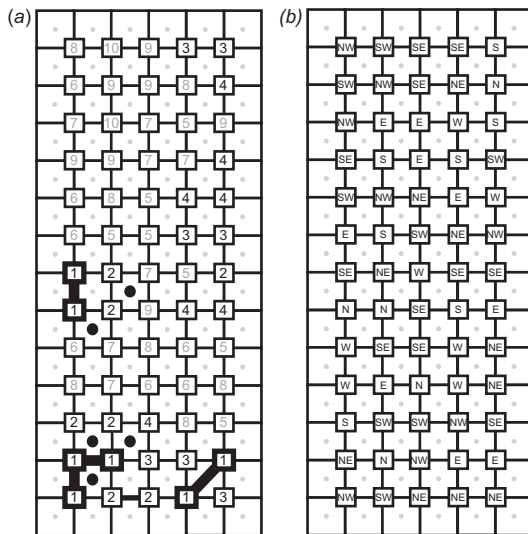


Figure 9.16 Lattice-wombling of abundance data for 26 tree species based on 84 sampling units (represented by squares with solid lines). (a) The 65 rates of change ($14_{\text{rows}} - 1 \times 6_{\text{columns}} - 1 = 13 \times 5$) are classified in 10 classes of 10th percentile each: the highest rate of change values are indicated by 1 and the lowest by 10. The candidate boundary elements are determined using the arbitrary threshold of the highest 10th percentile values (1 in bold) for a total of seven (rounded value). The bold lines link the candidate boundary elements that are spatially adjacent so that they can be connected into boundaries. There are three boundaries: two in the lowest part of the plot and one in the middle. The 10% highest second-derivatives (10% of 48 values = 5) are indicated by circles and they mark the end of the boundaries. (b) Orientation associated with each rate of change classified in eight directions (N, north; NE, northeast; E, east; SE, southeast; S, south; SW, southwest; W, west; and NW, northwest).

which considers the degree of spatial structure in the data, is therefore recommended (Fortin & Jacquez 2000). Also, when several variables are analysed, one could determine whether the candidate boundary elements are significant using a binomial test (Barbujani & Sokal 1991; Fortin 1994). This tests the significance of each candidate boundary element separately from all the other candidate boundary elements. For example, using the arbitrary threshold of the 10th percentile, each rate of change has a probability $p =$

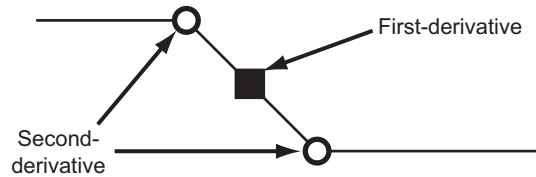


Figure 9.17 Lattice-wombling first derivatives identify boundary as the magnitude of the slope of a plane (square), whereas the second derivatives identify the inflection point where the boundary ends (circle). The bold lines link the candidate boundary elements that are spatially adjacent so that they can be connected into boundaries.

0.1 of being classified as a candidate boundary element. If a variables out of b variables analysed are candidate boundary elements at a given locality, the probability that this location is overall significant for the rates of change of all the variables is given by a binomial test:

$$\Pr(a|b) = \binom{b}{a} 0.1^a 0.9^{b-a}, \quad (9.24)$$

where $\binom{b}{a}$ is the number of possible ways to choose a elements out of b . The location is said to be significant when the binomial probability of the actual count a , given the maximum possible number b , is less than or equal to the 5% level. To test whether connected candidate boundary elements form cohesive boundaries, boundary statistics should be used (Section 9.3).

Finally, there are cases when the bilinear algorithm will not be able to provide accurate estimates of the gradient among the four adjacent sampling location values. For example, when two diagonal values are high and two others are low, hence creating a saddle shape (Figure 9.15), the gradient computed at the centroid point will misrepresent the data behaviour at those four sampling locations. Also, depending on the degree of spatial autocorrelation within patches, some boundaries may fall within patches, which makes the detection of cohesive ecological boundaries among patches more difficult (Csillag *et al.* 2001). One way to minimize within-patch boundaries and to maximize detection of between-patch boundaries is to carry out boundary detection at

several spatial resolutions of the sampling units. Such scaling procedures allow identification of the degree of boundaries' persistence across scales (Fortin 1999b; Csillag *et al.* 2001; Handcock & Csillag 2002; Philibert *et al.* 2008).

9.2.4.2 Non-lattice data: triangulation-wombling

In the field, ecological data are rarely completely surveyed on a lattice but rather data are sampled where the sampling locations are irregularly spaced. With such a data set, lattice-wombling cannot be carried out unless the data are initially interpolated onto a regular lattice. This is not recommended, however, because as presented in Chapter 6 most interpolation techniques smooth out the data, which in turn can diminish the strength of boundaries. Fortin (1994) proposed the use of a triangular window instead of a square one, where the three nearby sampling locations can be determined by using a Delaunay triangulation algorithm that links sampling locations on the basis of triangles (Chapter 3). By doing so, a plane can be fitted to the values of a variable observed at the vertices of the triangle. The magnitude of rate of change, m , based on the values of the three nearest sampling locations 1, 2, and 3 forming a triangle, is computed using the same equation as the one for lattice-wombling (Eq. (9.20)), but where $f(x, y)$ is

$$f(x, y) = ax + by + c, \quad (9.25)$$

and

$$\begin{bmatrix} a \\ b \\ c \end{bmatrix} = \begin{bmatrix} x_1 & y_1 & 1 \\ x_2 & y_2 & 1 \\ x_3 & y_3 & 1 \end{bmatrix}^{-1} \begin{bmatrix} z_1 \\ z_2 \\ z_3 \end{bmatrix}. \quad (9.26)$$

The position of the centroid is at the location

$$\left(\frac{x_1 + x_2 + x_3}{3} \right), \left(\frac{y_1 + y_2 + y_3}{3} \right). \quad (9.27)$$

As for the lattice-wombling algorithm, the average rate of change can be computed as well as the orientation of the rates of change with Eq. (9.22). By using a triangle instead of a square window, the saddle problem that can occur with the square window is impossible (Figure 9.18). On the other hand, when the four

nearest sampling locations are laid out as a perfect square, there are two possible combinations of triangles that can be selected, two triangle windows need to be selected (arbitrarily or not) for the analysis. When the four values are more or less similar, the selection of two triangles instead of two others will not have a big impact. However, if one or two values are very high and the others not, the rates of change will differ greatly and may affect the detection of boundaries.

The triangulation-wombling results based on a subset of 42 sampling locations from the 84 original ones (Figure 9.16) are shown in Figure 9.19. The triangulated systematic sampling design of the 42 sampling locations facilitates the visualization of the 64 triangle windows that were identified by the Delaunay connectivity algorithm (grey dashed lines in Figure 9.19). As in lattice-wombling, the number of calculated rates of change is smaller than the number of sampling locations, however, unlike lattice-wombling, there is no formula to evaluate this number because the number of triangles depends on the spatial arrangement of the sampling locations but it is usually around six neighbours (Chapter 3). The candidate boundary elements, based on the highest 10th percentile (i.e. 10% of 64 triangles = 6), are all connected and located in the lower left part of the study area. Therefore, both lattice- and triangulation-wombling are congruent in their detection of boundaries (Fortin & Drapeau 1995).

9.2.4.3 Categorical-wombling

It is common to have species presence: absence data over a two-dimensional area. In such cases, boundaries are located where there is high species turnover. These boundaries can be established using either spatial clustering as mentioned in Section 9.1.2, or by computing a match-mismatch measure between adjacent sampling locations (Oden *et al.* 1993). This last method is known as categorical-wombling (Oden *et al.* 1993; Fortin & Drapeau 1995), where mismatch values between adjacent sampling locations (i.e. not the same species in adjacent sampling locations or one species present in one sampling location and absent in another) are summed over all the

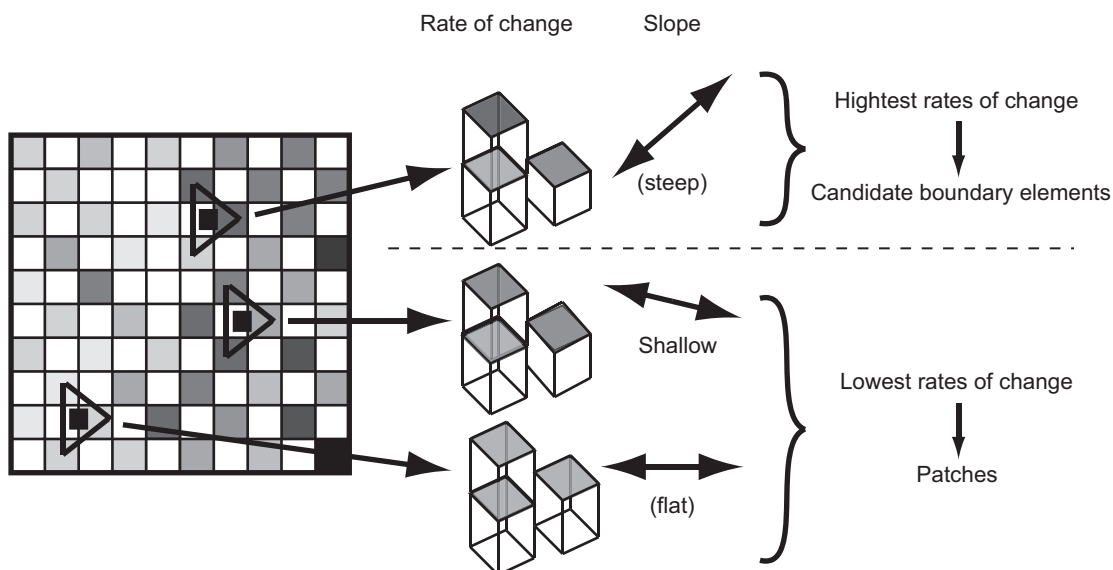


Figure 9.18 Triangulation-wombling algorithm. Rates of change based on triangulation-wombling are the slope of the plane that fits the three values of the variable at the sampling locations: the three locations are based on the Delaunay triangulation algorithm. The orientation of the slope could also be useful in some studies. When the rates of change are ranked in decreasing order of magnitude (highest values of the slope), the candidate boundary elements are determined using an arbitrary threshold. When the rates of change are very low, close to zero, the sampling locations are most likely part of a patch.

categorical variables (here species). Adjacent sampling locations can be obtained using any connectivity algorithm (Chapter 3). The number of mismatches can be ranked as with the lattice-wombling and triangulation-wombling algorithms and the highest values are represented at the midpoint between the linked sampling locations (Figure 9.20). Here there are 105 Delaunay links for a total of 11 theoretical candidate boundary elements, that is the highest 10th percentile. However, because several of the rates of change are similar, there are actually 17 candidate boundary elements for this set of data. Given that the number of elements of candidate boundaries is higher than the two previous wombling methods (categorical-wombling = 17, lattice-wombling = 7 and triangulation-wombling = 6), boundaries are detected not only in the lower part of the study area but also in the middle.

When we want to find boundaries using only presence : absence data of one species (e.g. species geographical range limit), the categorical-wombling

method is not appropriate and instead home-range delimitation methods based on kernel approaches should be used. We will not present these home-range methods here but refer the reader to Blundell *et al.* (2001) among others.

9.2.4.4 Other boundary detection methods

Several other boundary detection methods have been developed in the recent years ranging from Bayesian point wombling (Liang *et al.* 2009) for spatial point processes, Bayesian areal wombling (Lu & Carlin 2005; Fitzpatrick *et al.* 2010) for polygons instead of points, to the simultaneous local boundary detection and global spatial clustering methods proposed by Jacquez *et al.* (2008) based on a probabilistic framework. Also the Canny algorithm for lattice data can detect boundaries while accounting for local noise in the data (Canny 1986; Richardson *et al.* 2009).

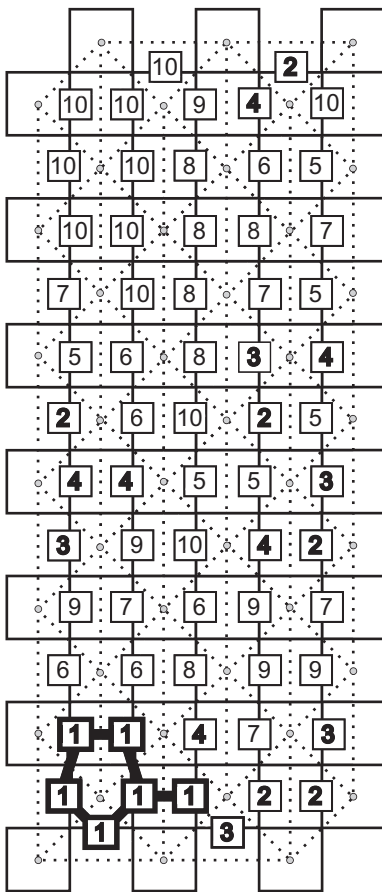


Figure 9.19 Triangulation-wombling of abundance data for 26 tree species based on 42 sampling units (represented by squares with solid lines). The 64 rates of change (one in each triangle that can be established using the Delaunay links – the dashed lines) are classified in 10 classes of 10th percentile each: the highest rate of change values are indicated by 1 and the lowest by 10. The candidate boundary elements are determined using the arbitrary threshold of highest 10th percentile values (1 in bold) for a total of six (rounded value). The bold lines link the candidate boundary elements that are spatially adjacent so that they can be connected into boundaries. There is only one boundary in the lowest part of the plot linking the six candidate boundary elements together. The locations of these boundaries coincide with those found with the lattice-wombling algorithm in Figure 9.16.

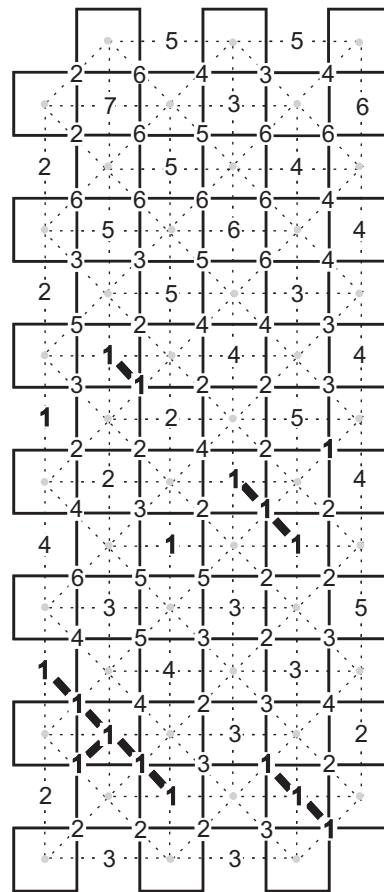


Figure 9.20 Categorical-wombling of presence-absence data for 26 tree species based on 42 units (represented by square with solid lines). The 105 rates of change (one for each Delaunay link – the dashed lines) are classified in 10 classes of 10th percentile each: the highest rates of change are indicated by 1 and the lowest by 10. The candidate boundary elements are determined by the arbitrary threshold of the highest 10th percentile values (1 in bold), theoretically giving 11 in total. However, because several of the rates of change are similar, there are actually 17 candidate boundary elements in total. The bold lines link the candidate boundary elements that are spatially adjacent so that they can be connected into seven boundaries: one in the lowest part of the plot linking six candidate boundary elements, three small boundaries (linking two or three candidate boundary elements) and three singletons (boundaries with only one candidate

9.3 Boundary statistics

Boundary detection techniques can be as subjective as spatial clustering methods: in the former, the researcher decides the rate-of-change threshold for candidate boundary elements; whereas in the latter, the researcher determines the degree of similarity and the number of clusters. To reduce the subjectivity in the choice of threshold and to test whether the candidate boundary elements at a given threshold form cohesive boundaries, Oden *et al.* (1993) developed sub-boundary statistics (hereafter referred to as boundary statistics). These boundary statistics try to capture the desirable properties of coherent boundaries formed from connected boundary elements (Fortin & Drapeau 1995; Bowersox & Brown 2001; Polakowska *et al.* 2012). The boundary properties include having fewer longer coherent boundaries (Figure 9.21a) that divide an area into patches (Figure 9.21b) and can be measured using the following boundary statistics.

- The number of boundaries: the number of connected subgraphs of candidate boundary elements (e.g. in Figure 9.21a there are four boundaries – A, B, C and D). When there are cohesive, coherent, boundaries in the study area, the number of boundaries should be low. When there are weak difference boundaries, the number of boundaries is high.
- The number of singletons: the number of isolated, unconnected candidate boundary elements (boundary with one element, D, in Figure 9.21a). When there are cohesive boundaries in the study area, the number of singletons should be low. When there are weak difference boundaries, the number of singletons is high.
- The maximum length of any boundary detected: the number of connected candidate boundary elements in the longest boundary (six candidate boundary elements in A, Figure 9.21a).

← **Figure 9.20** (*cont.*) boundary element) either in the lower or middle part of the plot. The locations of these boundaries coincide with the ones found with those of the lattice-wombling algorithm in Figure 9.16 and of the triangulation-wombling algorithm in Figure 9.19.

- The mean length of all the boundaries in the study area measured using: (i) the number of connected boundary elements $((6 + 3 + 3 + 1)/4 \text{ boundaries}) = 3.25$; or (ii) the number of edges connecting the boundary elements $((5 + 2 + 2 + 0)/4 \text{ boundaries}) = 2.25$.
- The maximum diameter among boundaries detected: the minimum distance, in connected candidate boundary elements, between the two most extreme locations of candidate boundary elements in a boundary (five candidate boundary elements in A, Figure 9.21a). The combination of the maximum length and maximum diameter is useful to discriminate among local and small discontinuities from more pronounced and cohesive boundaries.
- The mean diameters of all the detected boundaries measured using: (i) the number of connected boundary elements $((6 + 3 + 3 + 1)/4 \text{ boundaries}) = 3.25$; or (ii) the number of edges connecting the boundary elements $((5 + 2 + 2 + 0)/4 \text{ boundaries}) = 2.25$.
- The superfluity statistic: a measure of the efficiency of the boundaries to divide a study area into patches (i.e. the number of unnecessary rates of change, those whose removal does not change the number of patches) divided by the number of necessary rates of change that separate a study area into patches (those whose removal decreases the number of patches). The value of superfluity is low when there are only a few major cohesive boundaries because the majority of the rates of change will be necessary to divide an area into two, or more, patches. The value of superfluity is high when there are several weak differences and singleton boundaries dispersed throughout an entire study area so that the majority of the rates of change do not contribute to the partition into patches. In Figure 9.21b, the first boundary to separate the area into two patches contains seven rates of change and 11 were unnecessary ones (in ranking in descending order the rates of change, it took up to the 18th percentile to divide the area into two patches): the superfluity statistic is 0.63. The second boundary dividing the area into three patches (open circles, closed circles and closed squares) is formed of 20 rates of change and nine were unnecessary, giving a superfluity statistic of 0.45.

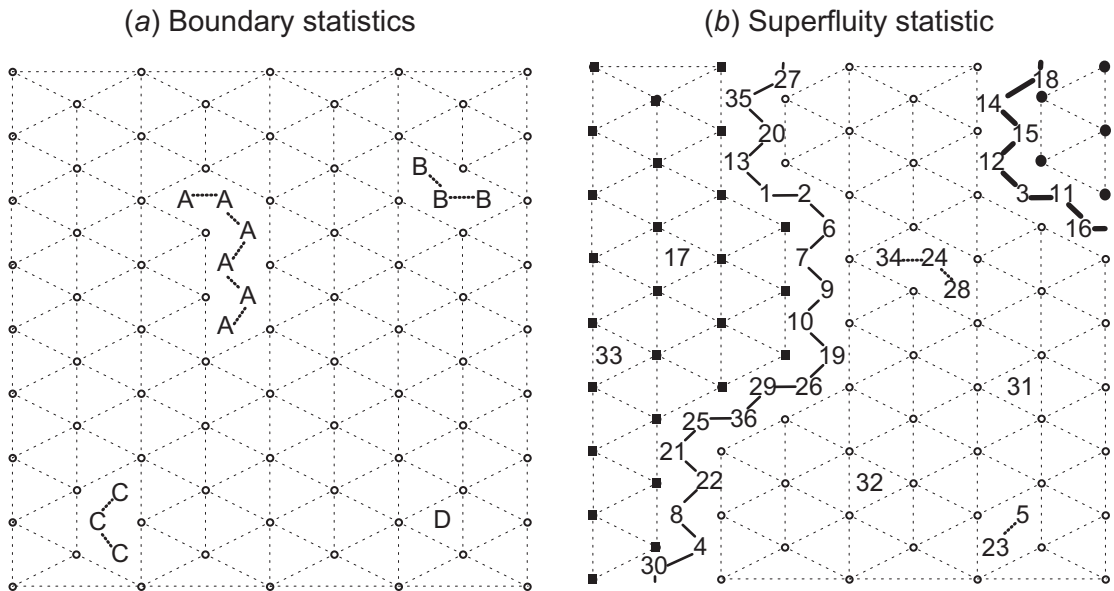


Figure 9.21 Boundary and superfluity statistics for 81 sampling locations (open circles). The Delaunay links are the dashed lines from which 128 triangles can be formed. Using the triangulation-wombling algorithm with a 10% threshold, there are 13 candidate boundary elements and boundary statistics as follows: (a) There are four boundaries (A, B, C and D) where one is a singleton (boundary D). The maximum length and maximum diameter are both for boundary A with six candidate boundary elements in length and five in diameter. The mean length and the mean diameter is 3.25 when measured using the number of connected boundary elements or 2.25 using the number of links. (b) To compute the superfluity statistic, the rates of change need to be ranked in decreasing order (1 being the highest). The first boundary that partitions the study area into patches is formed of only seven rates of change (bold lines) but it was necessary to go down the list to the rank of 18th percentile. The remaining 11 rates of change are part of the next boundary that divides the big patch into two and one rate of change is part of a difference boundary in the lower right part of the plot. The superfluity statistic for the first partition is 0.63 and for the second it is 0.45. To partition the study area into three patches (open circles, closed circles and closed squares) it was necessary to go down the list of rates of change to the 36th rank. The rates of change not part of the two partitioning boundaries are small difference boundaries or singletons.

Cohesive ecological boundaries will have significant boundary statistics that have extreme values: high ones for the number of boundaries, maximum length, maximum diameter, mean length and mean diameter and low ones for the number of singletons and the superfluity statistic. Significance tests assess whether the connected candidate boundary elements (i.e. boundaries) are likely to have occurred by chance or not. Oden *et al.* (1993) compared the two types of randomization procedures to assess the significance of the boundary statistics: a complete randomization test and a spatially restricted one considering the spatial structure of the data. They found that a null

distribution of boundary statistics generated from a random spatial pattern led to a conservative test that falsely rejected the null hypothesis fewer times than when tested using a spatially autocorrelated null distribution.

9.4 Boundary overlap statistics

Once cohesive boundaries have been delineated and their significance tested using boundary statistics, interesting ecological questions can be investigated using overlap statistics (Jacquez 1995; Fortin *et al.*

1996; St.-Louis *et al.* 2004; Fortin *et al.* 2005; Polakowska *et al.* 2012) that quantify the degree of spatial relationship between the locations of boundaries. Do boundaries directly overlap? Are boundaries spatially associated or do they repulse one another? In studying animal responses to forest boundaries, overlap statistics can be used to identify and to test which type of spatial relationships prevail. There are four overlap statistics; one measures the perfect spatial overlap between boundaries while the three others account for small spatial lags between the two boundaries due to sampling measurement errors.

- The direct overlap statistic, O_s , is the number of the candidate boundary elements that are at the same location. In Figure 9.22, $O_s = 7$.
- The mean minimum nearest distance statistic, O_1 , is an asymmetric measure of the distance from boundary 1 to boundary 2:

$$O_1 = \frac{\sum_{i=1}^{n_1} \min(d_i)}{n_1}, \quad (9.28)$$

where n_1 is the number of candidate boundary elements in boundary 1 and $\min(d_i)$ is the minimum Euclidean distance between the i th candidate boundary element of boundary 1 to a candidate boundary element of boundary 2. In Figure 9.22, the minimum distance between vegetation boundaries and animal boundaries is 15.5 units.

- The mean minimum nearest distance statistic, O_2 , is an asymmetric measure of the distance from boundary 2 to boundary 1:

$$O_2 = \frac{\sum_{j=1}^{n_2} \min(d_j)}{n_2}, \quad (9.29)$$

where n_2 is the number of candidate boundary elements in boundary 2 and $\min(d_j)$ is the minimum Euclidean distance between the j th candidate boundary element of boundary 2 to a candidate boundary element of boundary 1. In Figure 9.22, the minimum distance between animal boundaries and vegetation boundaries is 6.5 units.

- The overall mean minimum nearest distance statistic, O_{12} , between boundaries 1 and 2:

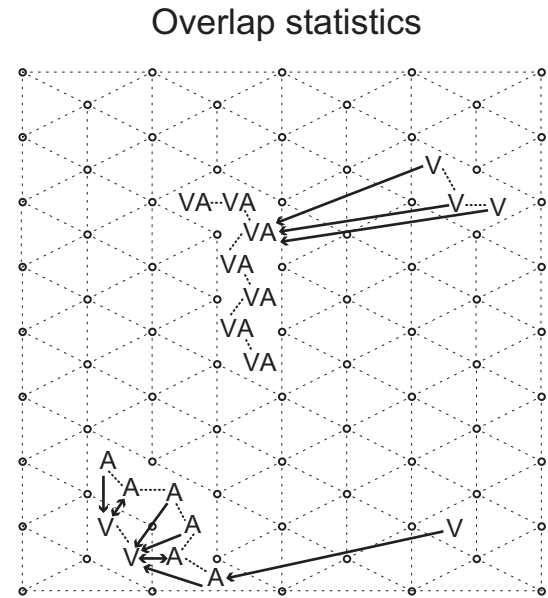


Figure 9.22 Overlap statistics between boundaries based on forest vegetation and animal abundance data for 81 sampling locations (open circles). The Delaunay links are the dashed lines from which 128 triangles can be formed. Using the triangulation-wombing algorithm with a 10% threshold, there are 13 candidate boundary elements for a total of four vegetation boundaries (indicated by V) and a total of two animal boundaries (indicated by A). The lines with an arrow at one end indicate the minimum nearest distances between the two types of boundaries (from one type to the other), while the lines with double arrows indicate the cases where the minimum nearest distances are symmetric in both directions. The overlap statistics are: O_s (direct overlap) is 7 candidate boundary elements (as indicated by the VA); the mean minimum nearest distance statistic, O_1 , is 15.5 units; the mean minimum nearest distance statistic, O_2 , is 6.5 units; and the overall mean minimum nearest distance statistic, O_{12} , is 11.0 units. This example illustrates well that the animal boundaries are closer to the vegetation ones than the reverse; suggesting that animal boundaries are spatially associated with vegetation boundaries, but that vegetation boundaries are not spatially associated with the animal boundaries.

$$O_{12} = \frac{\sum_{i=1}^{n_1} \min(d_i) + \sum_{j=1}^{n_2} \min(d_j)}{n_1 + n_2}. \quad (9.30)$$

In Figure 9.22, the overall mean minimum distance between the two boundaries is 11.0 units.

The statistic O_s allows us to test whether boundaries spatially coincide with one another, whereas the three other statistics, O_1 , O_2 and O_{12} , can help discriminate between boundaries that are spatially associated (small significant values) or repulsing one another (large significant values). To test the significant spatial relationship between boundaries, it is recommended to randomize the rates of change, rather than the raw data, because the rates of change already include the inherent spatial structure of each variable and that is what is of interest. As an example, candidate boundary elements (20% threshold) based on tree species and shrub species are mapped in Figure 9.23 as well as the minimum distance between them: O_s is 6 ($p = 0.1089$), O_{tree} is 8.6 m ($p = 0.0990$), O_{shrub} is 17.4 m ($p = 0.2178$) and $O_{\text{tree-shrub}}$ is 13.0 m ($p = 0.1188$). Although these overlap statistics are not significant, their trends indicate that the boundaries based on trees (8.6 m) are closer to those based on the shrubs (17.4 m). This indicates that tree-canopy opening due to gaps affect the spatial responses of both trees and shrubs, but that shrub changes (isolated singletons) do not affect trees.

The overlap statistics have been used to investigate the spatial relationship between forest edges and soil discontinuities (Fortin *et al.* 1996), as well as to test the relationship between bird and forest boundaries (Hall & Maruca 2001; St.-Louis *et al.* 2004) or landscape cover types (Polakowska *et al.* 2012). These overlap statistics offer a new means of investigating forest edge effects on other wildlife and environmental variables.

9.5 Hierarchical spatial partitioning

With only one quantitative variable (e.g. vegetation productivity based on the normalized difference vegetation index, NDVI), the lattice-wombling algorithm, being a local boundary detector, may not accurately detect a boundary, especially when there is local noise and spatial autocorrelation in the data. In such circumstances, hierarchical global edge detectors and kernel filters are more appropriate, and we will describe those next.

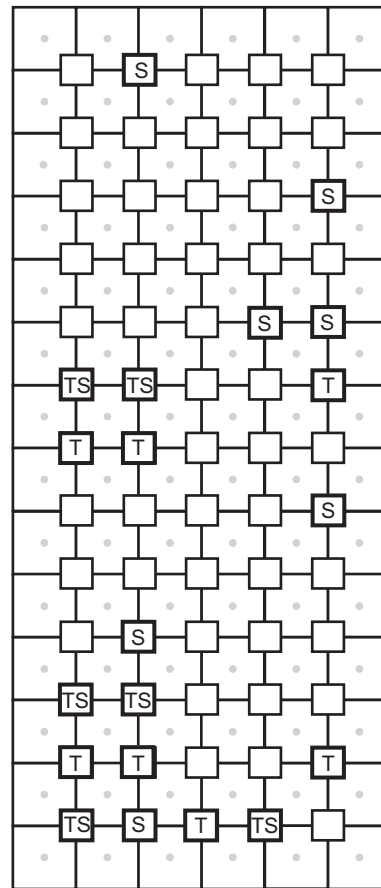


Figure 9.23 Overlap statistics between 26 tree species abundance and 9 shrub species abundance candidate boundary elements (using a 20% threshold) so a total of 13 based on the lattice-wombling algorithm and 84 sampling locations: O_s is 6 ($p = 0.1089$), O_{tree} is 8.6 m ($p = 0.0990$), O_{shrub} is 17.4 m ($p = 0.2178$) and $O_{\text{tree-shrub}}$ is 13.0 m ($p = 0.1188$). These results are not significant but can be used, combined with map observations, to indicate that tree-canopy gaps affect the spatial responses of both trees and shrubs but changes in shrubs (isolated singletons) do not affect trees.

A hierarchical global boundary detector, such as the wavelet transform analysis, can be used to identify boundaries from quantitative data along a transect (Redding *et al.* 2003; James *et al.* 2010) or an area (see Csillag & Kabos (2002) for mathematical details; James *et al.* 2011). In Chapter 5, wavelet variance was

introduced as a method to characterize and determine the scales of spatial patterns. Wavelet analysis is also used to compress an image to use less storage (Daubechies 1993) by using only a few wavelet transformation coefficients that can model the structure of relatively homogeneous subregions of an image. This feature can consequently be used to detect boundaries. This is achieved by partitioning and characterizing an image into relatively homogeneous areas using as many waveforms as are needed to model local pattern. Relatively homogeneous areas require few coefficients of low values whereas contrasting locations, such as edges, require more coefficients with larger values. Wavelet analysis allows local multiscale analysis of the data by partitioning the data into relatively homogeneous spatial subareas. The determination of these spatially homogeneous areas is obtained using a hierarchical procedure based on 'quadtree' decomposition (Csillag & Kabos 1996). Quadtree is a recursive algorithm that partitions an area into four initial quadrants and continues to divide each quadrant into four smaller quadrants in a hierarchical way until relatively homogeneous subareas are obtained. Depending on the spatial structure of the data, only one hierarchical partition will be sufficient to create a homogeneous subarea where a few wavelet transformation coefficients adequately describe the structure; while for other subareas, it will be necessary to add more partitions. The resulting subareas are often referred to as the leaves of the quadtree partition. The smallest possible leaf is the sampling unit itself. At each partition, wavelet transform coefficients are added to describe the structure and to indicate the level (scale) of partitions needed. For each leaf there is an equation. To obtain a higher degree of fit with the spatial pattern of data, more waveforms (wavelet transform coefficients) need to be kept at each partition level. For example, using the lattice-wombling of rates of change based on the abundance data for 26 tree species, the number of homogeneous areas increases when more coefficients are kept in the equation (Figure 9.24*a, b*). For image compression purposes, however, there is a trade-off between the amount of resolution retained and the storage of wavelet transformation coefficients at each scale and leaf. Usually more precision implies more

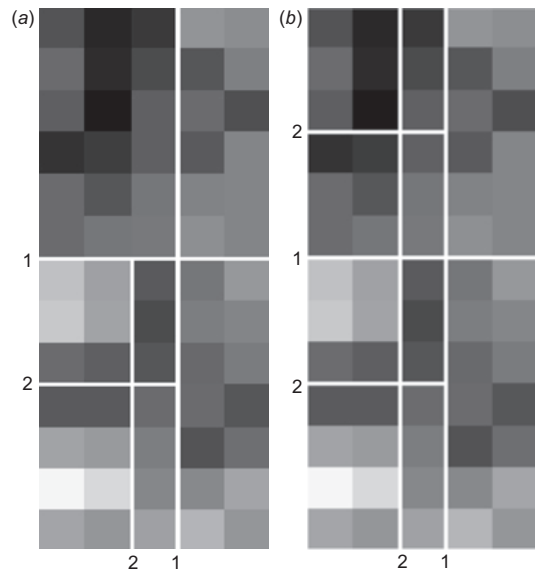


Figure 9.24 Spatial partition using the wavelet transforms at two hierarchical levels based on the rates of change of the lattice-wombling algorithm for the abundance data for 26 tree species (high values of rate of change are in white and low values in black): (a) seven subareas were found using only a few coefficients (10%) to describe the spatial structure in each; whereas in (b) 10 subareas were detected when using more coefficients (40%). Given the small sample size, only two partitions could be computed. Both in (a) and (b) the lower and middle of the plots show boundaries. When more coefficients are kept (b), other boundaries are identified in the upper left section of the plot.

leaves, thus more coefficients. Because the extent of the tree data is small ($13 \text{ rows} \times 5 \text{ columns} = 65 \text{ values}$), the partition cannot be performed for more than two hierarchical levels. Using black spruce percentage cover data over a larger region ($425 \text{ rows} \times 350 \text{ columns} = 148\,750 \text{ values}$), the partition can be extended up to the four hierarchical levels (Figure 9.25).

9.5.1 Edge enhancement with kernel filters

The kernel filters are local edge detectors used to enhance the contrast of the adjacent pixel of an image in order to detect the edges of objects. There are

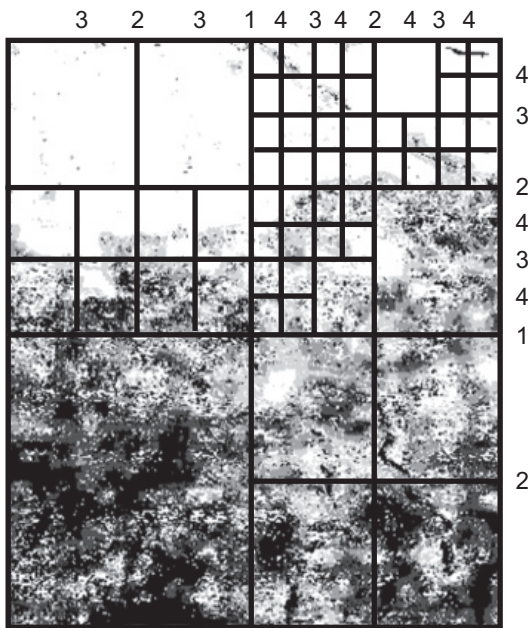


Figure 9.25 Spatial partition using the wavelet transforms at four hierarchical levels based on percentage coverage of black spruce in Quebec boreal forest (high values in white and low values in black). Most of the spatial partitions are in the upper right quadrant where the juxtaposition of high (white) and low (black) values necessitates more partition, i.e. coefficients, to describe the data. Indeed, trend patterns such as those seen in the upper left quadrant are easier to characterize than several small patches of low percentage coverage in forests of high percentage coverage.

several algorithms, called operators, which are available in most GIS and remote sensing software packages (Pitas 2000). The first ones to be developed aimed to measure the gradient on adjacent pixels using first- and second-order derivatives, such as the Laplacian filter. The 3×3 discrete approximation kernel version of the second-derivative Laplacian is:

$$\begin{bmatrix} 1 & 1 & 1 \\ 1 & -8 & 1 \\ 1 & 1 & 1 \end{bmatrix}, \quad (9.31)$$

where the sum of the kernel equals zero. Note that this Laplacian filter is the same as the template of the 9TLQV as in Figure 5.5. With such a filter, the resulting

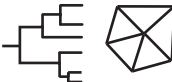


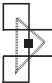




values are all zero except at the locations where an edge begins and ends, hence, boundaries are easier to detect. The major problem with the Laplacian operator, however, is that it is sensitive to noise, making it necessary to smooth the data first. Smoothing the data can be achieved either by aggregating adjacent cells, obtaining fewer larger cells (see Fortin 1999b), or by using a Gaussian filter that preserves the same number of cells. The most efficient kernel filters both reduce the noise and detect edges, such as the Canny adaptive filter (Canny 1986; Richardson *et al.* 2009) or the scale-space techniques using the Laplacian or Gaussian algorithm (Marr & Hildreth 1980; Lindeberg 1994; Faghih & Smith 2002). The scale-space techniques perform a series of smoothing using a Gaussian kernel of increasing size, allowing detection of the persistence of boundaries across scales. Figure 9.26 combines the smoothed data based on a Gaussian filter using a scaling factor of 40 cells and the delineated edges based on the Laplacian filter. Unlike the wavelet analysis that finds partitions based on the entire region (Figure 9.25), the scale-space approach identifies many more local boundaries because all the edges are mapped (Figure 9.26). As mentioned, the Laplacian algorithm localizes edges where the sum of the kernel is not zero. Thus, the boundaries can be either strong or weak, but will be treated similarly. Note that the use of overly large kernel size can distort the spatial partitioning by smoothing the data in an isotropic fashion. The scale-space approach has been used in forestry to identify individual trees in a forest from high spatial resolution aerial imagery data (Brandtberg 1999).

Several other kernels are available, such as non-linear kernels based on polynomials or global thresholding kernels. The reader interested in kernel filters should read the computer vision and image recognition literature applied to remotely sensed data and medical imagery.

9.6 Concluding remarks

Spatial partitioning based either on spatial clustering or boundary detection methods presented in this

Table 9.2 Summary of the spatial analysis methods presented in Chapter 9

Spatial analysis method	Template
Spatial clustering	
Moving split-window	
Lattice-wombling	
Triangulation-wombling	
Caterigorical-wombling	
Enhancement filter	
Wavelets	
Scale-space	

chapter are only the tip of the iceberg. Here we have focused only on the methods that have been developed, or are more commonly used, by ecologists (Table 9.2). There are, however, numerous other methods, mostly developed for image recognition, that enhance edges by smoothing and thresholding noise in an image. These sophisticated kernels are useful when only one variable is available. Caution is advised, however, because by seeking to smooth out noise using larger kernel sizes the spatial pattern can be deformed by imposing an isotropic shape.

In ecological contexts where several variables are used to detect ecotones or cohesive ecological boundaries, several conceptual and methodological aspects need to be addressed. From an ecological point of view, all variables and species may not all have the same weight in the detection of boundaries. Hence, rare or omnipresent species may not be as important as indicator species or species responding to specific

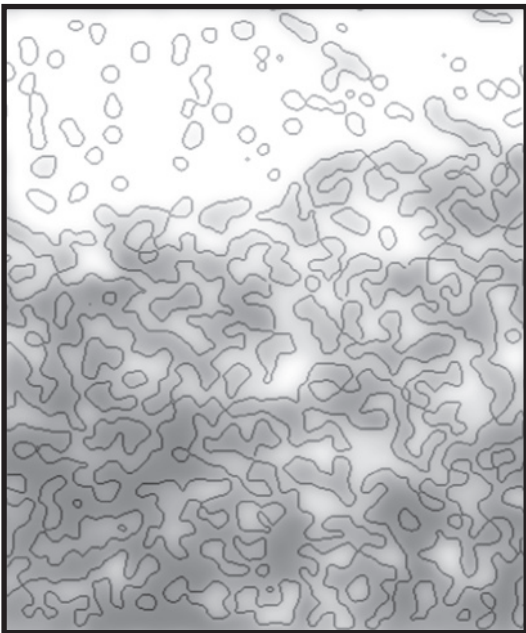


Figure 9.26 Spatial partition using the scale-space technique of the percentage coverage of black spruce in Quebec boreal forest as in Figure 9.25. First the data are smoothed using a Gaussian filter with a scaling factor of 40 cells (high values in white and low values in black) and then edges are delineated using a Laplacian filter (solid lines). All the edges are mapped without knowing which ones indicate the sharpest difference among cells.

environmental conditions. From a methodology perspective, novel ways to measure the spatial overlap between boundaries are needed so that we can compute the distance between a line boundary (vector mode) and a difference boundary (raster mode).

Finally, the most challenging issue to be addressed is the need to integrate both ecological concepts and statistical theory. What are the most appropriate ways to generate restricted randomization procedures that can test if boundaries are cohesive ones? Indeed, as presented above, complete spatial randomness is not an appropriate procedure to test the significance of rates of change, boundary statistics and overlap statistics. Restricted randomization that captures the spatial structure of the data is recommended. With

any ecological data, restricted randomization procedures need to reflect our ecological understanding of the processes. In the particular case of ecological boundaries, several processes are acting: the processes that created the patches and those that generated the boundaries. Usually, they are all different, or at least the processes that generated the patches on each side of the boundary that separates them are different. Consequently, a given study area where patches and boundaries occur is the perfect example of a non-stationary situation where global spatial statistics and global randomization cannot be performed. Hence we are in a 'chicken and egg' situation where

the proper way to restrict the randomization by area is first to identify these subareas having the same stationarity, but this is exactly what we are seeking by doing spatial partitioning. James *et al.* (2011) provided a first attempt to test boundaries detected based on wavelet using restricted randomization based on the spatial structure of the data using an autoregressive model and a Gaussian random field model. This restricted randomization approach shows a promising avenue to test the significance of boundaries using the empirical data. Other developments will require modelling of the processes that generated the boundaries.